

NBS-GCR-86-519

**FLUID-STRUCTURE INTERACTION EFFECTS  
FOR OFFSHORE STRUCTURES**

---

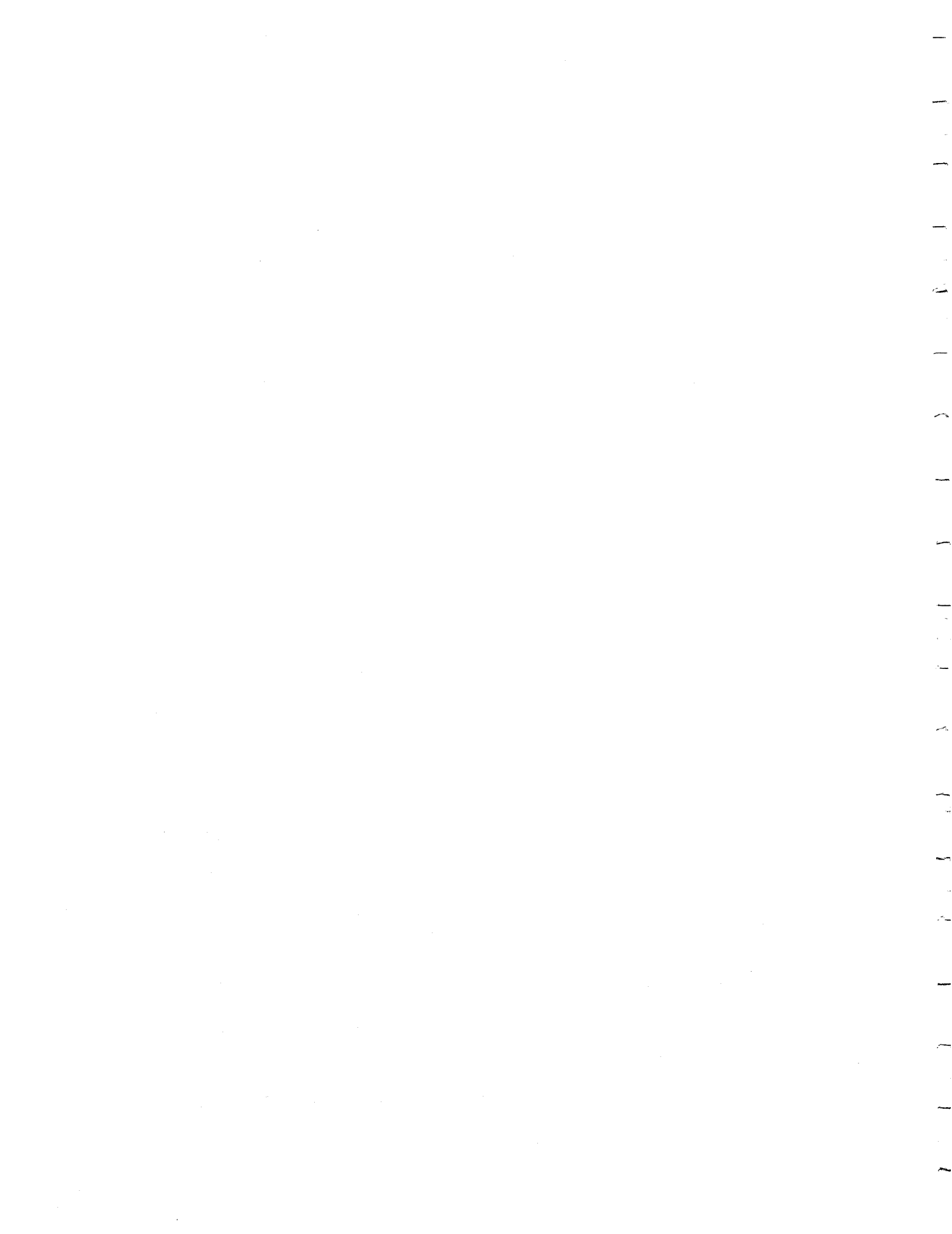
A. S. Veletsos, A. M. Prasad, and G. Hahn

Department of Civil Engineering  
Rice University  
Houston, TX 77251

October 1986

Issued December 1986

Prepared for  
Minerals Management Service  
Reston, Va 22091



## FOREWORD

The Technology Assessment and Research Branch of the Minerals Management Service (MMS), United States Department of the Interior, is engaged in a program of research and development to provide information on the performance of offshore systems. As part of this program, the MMS is sponsoring the project "Assessment of Uncertainties and Risks Associated with the Dynamic Response of Compliant Structures" under contract with the National Bureau of Standards (NBS).

Among these uncertainties are those related to the effects of the fluid-structure interaction on the structural response. The purpose of this report is to present information and procedures that allow these effects to be estimated readily in the case of simple offshore structure models. An approximation is proposed for the hydrodynamic modal damping factors of multi-degree-of freedom systems, which is particularly useful for preliminary design purposes.

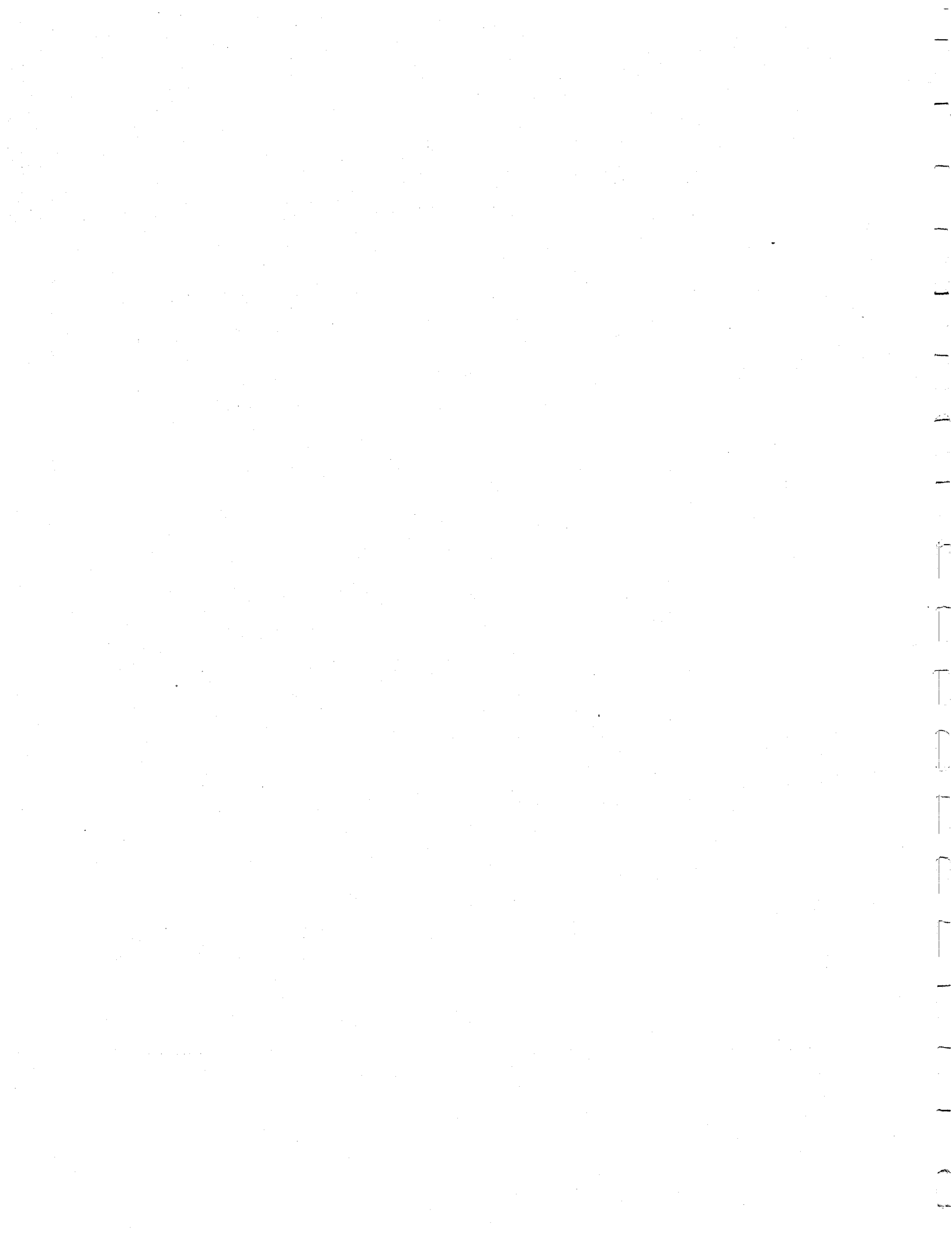
It is shown in the report that, in certain cases, the equivalent linearization technique can lead to substantial errors. (A similar conclusion was reached in a previous study sponsored by MMS, entitled "Response of Compliant Offshore Structures to Waves", NBS-GCR-85-501, September 1985.) The report also evaluates Penzien's decoupling technique, and notes its advantages over the equivalent linearization procedure. It then proposes a modification to this technique, which further improves

its accuracy.

Emil Simiu  
Structures Division  
Center for Building Technology  
National Bureau of Standards

## DISCLAIMER

The statements and conclusions contained in this report are those of the contractor and do not necessarily reflect the view of the U.S. Government and, in particular, the National Bureau of Standards or the Department of the Interior. Neither NBS or the contractors make any warranty, express or implied, or assume any legal liability or responsibility for the accuracy, completeness or usefulness of any information, apparatus, product or process disclosed or represent that its use would not infringe privately owned rights. They accept no responsibility for any damage that may result from the use of any information contained herein. The mentioning of manufacturers, professional firms, names, products, and the publication of performance data do not constitute any evaluation or endorsement by the U.S. Government, its agencies, or the contractor. It is done in a generic sense to illustrate particular points.



# FLUID-STRUCTURE INTERACTION EFFECTS FOR OFFSHORE STRUCTURES

by

A. S. Veletsos,<sup>1</sup> A. M. Prasad,<sup>2</sup> and G. Hahn<sup>3</sup>

**ABSTRACT:** Comprehensive analyses are made of the differences in the responses of simple models of offshore structures computed by the standard and extended versions of Morison's equation for the hydrodynamic forces, and of the effects and relative importance of the numerous parameters involved. The responses also are evaluated by the equivalent linearization technique and Penzien's decoupling technique, and the interrelationship and accuracy of these approaches are elucidated. The results are displayed graphically in the form of response spectra for absolute maximum displacement employing dimensionless parameters that are easy to interpret and use. In addition, the decoupling technique is generalized to include consideration of a current of constant velocity, and a simple modification is proposed which improves the accuracy of this approach. A particularly simple approximation is included for the hydrodynamic modal damping values of multi-degree-of-freedom, stick-like systems.

---

<sup>1</sup>Brown & Root Prof., Dept. of Civ. Engrg., Rice Univ., Houston, TX 77251

<sup>2</sup>Graduate Student, Dept. of Civ. Engrg., Rice Univ., Houston, TX 77251

<sup>3</sup>Formerly Graduate Student, Dept. of Civ. Engrg., Rice Univ., Houston, TX 77251

## INTRODUCTION

Wave forces on an offshore structure are normally computed by one of the following variants of Morison's equation: (1) the standard version, in which the structure is effectively presumed to be rigid and the drag components of the wave forces are taken proportional to the square of the fluid particle velocities; and (2) the generalized or extended version, in which the drag force components are considered to be proportional to the square of the relative velocities of the fluid and structure. The difference in the responses of a structure computed by these two representations of the forcing function will be referred to herein as the fluid-structure interaction effect.

In a direct, numerical evaluation of the response of the structure as a function of time, there is no fundamental difficulty in providing for these effects. This approach, however, is generally too tedious and costly for preliminary design purposes, and simpler techniques are needed to define the conditions under which the effects are of sufficient importance to warrant their consideration in design and to evaluate them reliably and cost-effectively. Two such techniques have already appeared in the literature. They are: (1) the Malhotra-Penzien extension [4,8]\* of Borgman's linearization technique for the drag component of the exciting force [2]; and (2) Penzien's decoupling technique [11,12].

Notwithstanding these and several other contributions [3,4,9,14,15], there is a need for a reexamination of the problem from a unified point of view, and for a critical assessment of the effects of the numerous factors involved. This report is intended to be responsive to this need.

---

\*Numbers in brackets refer to the corresponding items in the list of references in Appendix II.

Its objectives are: (1) To elucidate the nature of the fluid-structure interaction phenomenon; (2) to assess the interrelationship, accuracy and ranges of applicability of the previously proposed simple procedures for evaluating its effects; and (3) where necessary, to recommend appropriate improvements.

Comprehensive parametric studies are made of the exact maximum responses induced in simple mass-spring-dashpot systems by several different combinations of a simulated wave train and a constant-velocity current, and the results are compared with those obtained by the previously proposed approximate procedures or appropriate extensions of them. The problem parameters examined include the natural frequency and percentage of critical damping of the system, the relative magnitudes of the drag and inertia components of the exciting force, the ratio of the current velocity to the peak value of the wave-induced fluid particle velocity, and a dimensionless measure of the importance of fluid-structure interaction. The results are displayed in the form of response spectra for the absolute maximum displacement of the system. It is shown that the accuracy of the approximate techniques depends importantly on the relative magnitudes of the drag and inertia components of wave loading, and that these procedures may lead to substantial errors under certain conditions. The reasons for these discrepancies are identified, and simple modifications are proposed which improve the reliability of these techniques.

In addition to the response of single-degree-of-freedom systems, the response of multi-degree-of-freedom cantilever systems is examined, and a simple approximation is proposed for the effective modal damping of such systems.

Although the reliability of both the standard and extended versions

of Morison's equation has been questioned [7,13], their use in practice is so widespread that it is considered important that the interrelationship of the responses corresponding to the two forms of this equation be clarified.

### STATEMENT OF PROBLEM

Consideration is first given to the response of single-degree-of-freedom, mass-spring-dashpot systems submerged in an oscillating fluid for which the particle velocity is  $\dot{u}(t) = \dot{u}$  and the associated acceleration is  $\ddot{u}(t) = \ddot{u}$ . Let  $m$  be the effective mass of the system, including the contribution of added fluid mass, and let  $k$  and  $c$  be its stiffness and coefficient of damping, respectively.

With the hydrodynamic force defined by the generalized version of Morison's equation, the equation of motion for the system may conveniently be expressed in the form

$$m\ddot{x} + c\dot{x} + kx = P_i \frac{\ddot{u}}{\ddot{u}_0} + P_d \frac{|\dot{u} - \dot{x}|}{\dot{u}_0} \frac{(\dot{u} - \dot{x})}{\dot{u}_0} \quad (1)$$

in which  $x$  denotes the displacement of the system; a dot superscript denotes differentiation with respect to time;  $\ddot{u}_0$  and  $\dot{u}_0$  are the absolute maximum values of  $\ddot{u}$  and  $\dot{u}$ ; and  $P_i$  and  $P_d$  are the corresponding values of the inertia and drag components of the exciting force computed without regard for interaction. The latter values are given by

$$P_i = C_m \rho V \ddot{u}_0 \quad (2a)$$

$$\text{and } P_d = \frac{1}{2} C_d \rho A \dot{u}_0^2 \quad (2b)$$

in which  $C_m$  and  $C_d$  are the inertia and drag force coefficients;  $\rho$  = the mass density of the fluid; and  $V$  and  $A$  are the volume and projected area

of the system, respectively. The coefficients  $C_m$  and  $C_d$  are presumed to be constants.

Of concern here is the difference in the responses of the system computed on the following bases: (1) Considering  $P(t)$  to be defined by the right-hand member of Eq. 1; and (2) using the following simpler expression for it

$$P(t) = P_i \frac{\ddot{u}}{\ddot{u}_0} + P_d \frac{|\dot{u}|}{\dot{u}_0} \frac{\dot{u}}{\dot{u}_0} \quad (3)$$

Of particular interest is the difference in the absolute maximum values of the resulting displacements,  $|x_{\max}|$ . These displacements will be normalized with respect to  $x_{st}$ , the static displacement induced by the peak value of the wave loading. The interaction effects for more complex, multi-degree-of-freedom systems are examined at the end of the paper.

#### PROBLEM PARAMETERS

The normalized response of the system to a prescribed sea state depends on the following parameters: (1) The relative magnitudes of the drag and inertia components of the exciting force, expressed conveniently by the factor

$$\alpha = \frac{P_d}{P_i + P_d} \quad (4)$$

(2) the dynamic properties of the system, including its natural frequency,  $f$ , and the percentage of critical damping,  $\zeta$ ; and (3) the dimensionless interaction parameter defined by

$$\delta = \frac{\omega(x_{st})_d}{\dot{u}_0} \quad (5)$$

in which  $\omega = 2\pi f$  = the circular natural frequency of the system; and  $(x_{st})_d = P_d/k$  = the static displacement induced by the peak value of the drag component of the wave loading. The parameter  $\delta$  is deduced readily from Eq. 1 by expressing the latter in terms of the dimensionless time,  $\tau = \omega t$ , and by normalizing  $x$  in terms of  $(x_{st})_d$ . A value of  $\delta = 0$  refers to a noninteracting system. One of the distinguishing features of the present study, the use of the dimensionless factors  $\alpha$  and  $\delta$  greatly simplifies the interpretation and use of the data presented herein.

### SEA STATE CONSIDERED

A simulated sea state, generated from a one-dimensional Pierson-Moskowitz wave spectrum in combination with linear wave theory, is considered. The total depth of water is presumed to be 800 ft; the significant height and mean period of the waves are taken as 40 ft. and 12.4 sec., respectively; the ordinates of the wave spectrum for frequencies in excess of 0.4 cps are assumed to be zero; and the phase angles for the component harmonics were taken as random numbers uniformly distributed between zero and  $2\pi$ . The wave spectrum was sampled at increments of 0.004883 cps for a total of 2048 points. This leads to wave trains that are defined at time increments of 0.1 sec and repeat at intervals of 204.8 sec. All wave forces were computed from the fluid kinematics of this sea state at a depth of 40 ft. beneath the mean water level. The relevant histories of the horizontal components of the fluid particle velocity and acceleration are shown in Fig. 1 normalized to a unit peak value.

### PRINCIPAL EFFECTS OF INTERACTION

The natural and most direct means of assessing the consequences of fluid-structure interaction would be to compare the histories of the

exciting forces and of the corresponding responses computed from Eqs. 1 and 3.

Such comparisons are presented in Figs. 2 and 3 for systems with  $f = 0.1$  cps and  $f = 0.2$  cps subjected to a purely drag component of wave loading ( $\alpha = 1$ ). The damping factor of the systems in these solutions was taken as  $\zeta = 0.02$ . The solid lines in the top two diagrams in each of these figures represent the solutions obtained without regard for interaction, and the dashed lines represent the corresponding solutions obtained with due provision for interaction assuming that  $\delta = 0.10$ . Also shown in expanded scales are the histories of the differences in the two sets of results. The force histories are normalized with respect to  $P$ , the peak value of the total exciting force for no interaction, and the displacement histories are normalized with respect to the corresponding static displacement,  $x_{st}$ . All system responses were evaluated by numerical integration of the governing equation of motion for a single cycle of the forcing function, using an integration step of 0.1 sec. and considering the structure to be initially at rest.

It can be seen that fluid-structure interaction modifies both the exciting force and the resulting response, generally reducing the absolute maximum values of these quantities. The change in the exciting force,  $\Delta P(t)$ , is generally quite small, particularly when the natural frequency of the system is substantially different from the dominant frequency of the excitation, as is the case in Fig. 3. By contrast, the change in response,  $\Delta x(t)$ , is generally significant. This is due to the fact that  $\Delta P(t)$  is an oscillatory, nearly periodic force component with a dominant frequency equal to the natural frequency of the system under consideration and it induces a resonant-like component of response.

Critical analysis of these data further reveals that there is approxi-

mately a  $90^\circ$  phase difference between  $\Delta P(t)$  and  $\Delta x(t)$ . This suggests that the mechanism of fluid-structure interaction is similar in its effect to that of linear viscous damping, and that it tends to reduce the absolute maximum displacement of the system,  $|x_{\max}|$ . It further suggests that the reduction in response would be particularly significant at natural frequencies close to the dominant frequency of the exciting force.

Although comparative studies of the type presented in Figs. 2 and 3 provide valuable insight into the mechanism of fluid-structure interaction, they are not particularly convenient for quantifying the effect of this action on the maximum response of the system, and the alternative approaches examined in the following sections are preferable. Clearly, there is no simple correlation between the change in the exciting force and the corresponding change in response. In particular, the change in the peak value of the exciting force is generally a poor indicator of the corresponding change in peak response. This is clearly shown in Table 1, in which dimensionless measures of  $|P_{\max}|$  and  $|x_{\max}|$  for several different values of  $f$  and  $\alpha$  are listed for both non-interacting systems ( $\delta = 0$ ) and for interacting systems with  $\delta = 0.10$ . Note that the effect of interaction on both  $|P_{\max}|$  and  $|x_{\max}|$  is highly sensitive to the values of  $f$  and  $\alpha$  involved.

#### EQUIVALENT LINEARIZATION TECHNIQUE

The velocity squared term in the expression for the drag component of the exciting force in this approach is approximated by a linear term [8] as

$$|(\dot{u} - \dot{x})|(\dot{u} - \dot{x}) \approx 2 b_0 \dot{u}_0 (\dot{u} - \dot{x}) \quad (6)$$

in which  $b_0$  is a dimensionless factor determined so as to minimize the

temporal average of the square of the resulting error. The latter factor is given by

$$b_0 = \frac{1}{2u_0} \frac{\langle |\dot{u}-\dot{x}|^3 \rangle}{\langle (\dot{u}-\dot{x})^2 \rangle} \quad (7a)$$

in which  $\langle \cdot \rangle$  denotes the temporal average of the enclosed quantity. The coefficient 2 on the right-hand member of Eq. 6 is included for convenience in relating the results of this approximation to those of the decoupling technique presented later. For a normal random wave (one for which the fluid kinematics is represented by a Gaussian random process), Eq. 7a reduces to

$$b_0 = \sqrt{\frac{2}{\pi}} \frac{\sigma_{\dot{u}-\dot{x}}}{\dot{u}_0} \quad (7b)$$

in which  $\sigma_{\dot{u}-\dot{x}}$  is the standard deviation of the relative velocity of the fluid and structure.

On introducing the approximation defined by Eq. 6 into Eq. 1, and transposing to the left-hand member of the equation the term involving the structural velocity, one obtains

$$m\ddot{x} + (c + c_0)\dot{x} + kx = P_i \frac{\ddot{u}}{\dot{u}_0} + 2b_0 P_d \frac{\dot{u}}{\dot{u}_0} \quad (8)$$

in which

$$c_0 = \frac{2b_0 P_d}{\dot{u}_0} \quad (9)$$

Fluid-structure interaction according to this approximation has a two-fold effect: (1) It modifies the drag component of the exciting force to a linear function of the fluid particle velocity; and (2) it increases the damping of the system.

When expressed in percent of the critical damping coefficient,  $c_{cr} = 2m\omega$ , the effective damping of the system,  $\tilde{\zeta} = (c + c_0)/c_{cr}$ , is given by

$$\tilde{\zeta} = \zeta + \zeta_0 = \zeta + b_0 \delta \quad (10)$$

in which use has been made of Eq. 5. The quantities  $\zeta$  and  $\zeta_0$  represent the contributions of the structural damping and of the added hydrodynamic damping, respectively.

The dimensionless factor  $b_0$  in Eqs. 8, 9 and 10 is a function of the response of the system, and must therefore be computed by iteration. The process is typically started with the value of  $b_0$  corresponding to  $\dot{x} = 0$ . The response of the system is then computed and a new value of  $b_0$  is determined. These steps are repeated until the difference between the starting and derived values is less than a prescribed tolerance.

**Results for Noninteracting Systems.** — Valuable insight into the accuracy of the linearization technique may be gained from an analysis of the response of non-interacting systems, for which the procedure reduces to that originally proposed by Borgman [2]. In this case, the structural velocity in Eq. 6 and hence the term involving the damping coefficient  $c_0$  in Eq. 8 vanish, and Eqs. 7a and 7b reduce to

$$b_0 = \frac{1}{2\dot{u}_0} \frac{\langle |\dot{u}|^3 \rangle}{\langle (\dot{u})^2 \rangle} \quad (11a)$$

$$\text{and } b_0 = \sqrt{\frac{2}{\pi}} \frac{\sigma_{\dot{u}}}{\dot{u}_0} \quad (11b)$$

respectively.

The exact and approximate values of  $|x_{max}|$  induced in systems with  $\zeta = 0.02$  by several different combinations of the drag and inertia components of the simulated wave loading are compared in Fig. 4. The results

are displayed in the form of response spectra. Not to be confused with a wave spectrum which characterizes the excitation, a response spectrum defines the maximum response to a specified excitation of a family of single-degree-of-freedom systems having different natural frequencies. A rather broad range of natural frequencies and values of  $\alpha$  in the range between 0.25 and unity are considered. The normalizing displacement,  $x_{st}$ , in these plots, as in Figs. 2 and 3, represents the static displacement induced by the peak value of the actual wave force, not of its linearized approximation.

The exact responses were computed by direct integration of Eq. 1 considering the system to be initially at rest, and the approximate responses were obtained by the linearization technique using the value of  $b_0 = 0.266$  determined from Eq. 11a. For comparison, the value computed from Eq. 11b for a normal random wave is the same, whereas the value obtained for a single harmonic wave is  $b_0 = 0.424$ .

As would be expected, the accuracy of the approximate solution depends importantly on the value of the load factor,  $\alpha$ . The larger this factor, the greater is the part of the response contributed by the drag component of the exciting force, and hence the greater is the consequence of the approximations involved in the linearization technique. For a specified value of  $\alpha$ , the agreement between the approximate and exact solutions can be seen to be excellent in the central region of the response spectrum which is associated with a resonant-like response and large amplification factors. The agreement also is good in the low-frequency spectral region for which the response is generally not sensitive to the amount of damping involved. By contrast, there are significant and consistent differences in the practically important, right-hand region of the spectrum which

covers the typical range of natural frequencies for fixed-base offshore platforms.

The latter differences stem from the inability of the linearization technique to represent adequately the high frequency force components to which high-frequency systems are sensitive. This fact is also reflected in the high-frequency limits of the response spectra. Considering that very stiff systems respond as if they were statically loaded, the right hand limits of the spectra must be proportional to the absolute maximum value of the exciting force under consideration,  $|P_{\max}|$ .

The exact and approximate values of this force are listed in Columns 2 and 3 of Table 2 for several different values of the load factor,  $\alpha$ . The results are normalized with respect to  $P_i + P_d$ , the numerical sum of the peak values of the component forces, with  $P_d$  taken as the peak value of the exact drag force. Note that the difference between the exact and approximate values of  $|P_{\max}|$  increases with increasing  $\alpha$ . It is of interest to note further that  $|P_{\max}|$  is substantially less than  $P_i + P_d$ . This is, of course, due to the fact that the peak values of the inertia and drag force components occur at different times.

**Results for Interacting Systems.** — The results for the noninteracting systems presented in Fig. 4 suggest that the linearization technique should lead to similar errors for interacting systems as well. That this is indeed the case is demonstrated by the spectra in Figs. 5 which refer to systems with  $\zeta = 0.02$  and three different values of the load factor,  $\alpha$ . The interaction parameter in these solutions is taken as  $\delta = 0.10$ ; in reality, low-frequency systems are likely to be associated with larger values of  $\delta$  than high frequency systems.

Similar data are presented in Fig. 6 for systems which in addition to the wave loading are acted upon by a current of constant velocity,  $\dot{u}_c = 0.5\dot{u}_0$ . The normalizing displacement,  $x_{st}$ , in these plots represents, as in Fig. 4, the static displacement induced by the peak value of the wave component of loading, not of the combination of wave and current. Similarly, the value of  $\delta$  is expressed in terms of the  $(x_{st})_d$  corresponding to the wave loading only.

The solutions by the linearization technique were obtained in the manner indicated in Ref. 15 by: (1) Replacing the wave-induced fluid velocity,  $\dot{u}$ , in Eq. 8 by the total velocity

$$\dot{v} = \dot{u}_c + \dot{u}; \quad (12)$$

(2) determining the factor  $b_0$  in Eqs. 8 and 9 from the following generalized version of Eq. 7a

$$b_0 = \frac{1}{2\dot{u}_0} \frac{\langle |\dot{v}-\dot{x}| (\dot{v}-\dot{x})(\dot{u}-\dot{x}) \rangle}{\langle (\dot{u}-\dot{x})^2 \rangle}; \quad (13)$$

and (3) interpreting  $x$  to be the displacement measured from the mean value of the resulting total displacement. Denoted by  $x_0$ , the mean displacement is given by

$$x_0 = \frac{\langle |\dot{v}-\dot{x}| (\dot{v}-\dot{x}) \rangle}{\dot{u}_0^2} (x_{st})_d. \quad (14)$$

With  $x$  computed in this manner, the total displacement is obtained by superimposing the value  $x_0$ . The exact solutions were computed from Eq. 1 by replacing  $\dot{u}$  by  $\dot{v}$ ; and to avoid the spurious oscillations in the response due to the initial discontinuity of the current loading, the equation was rewritten in terms of  $x - x_c$ , in which  $x_c$  = the static displacement due to the current-induced loading.

Note that even for  $\dot{u}_c/\dot{u}_0 = 0.5$ , for which only a relatively small fraction of the total loading gets approximated in the linearization technique, the errors in response may be significant in the high-frequency region of the response spectra. The maximum values of the exact and linearized versions of the exciting forces are listed in Columns 4 and 5 of Table 2 along with those corresponding to  $\dot{u}_c/\dot{u}_0 = 1$ . The high-frequency limits of the response spectra in Fig. 6 are, of course, proportional to these force values.

**Convergence of Procedure.** — The iterative process required to compute the factor  $b_0$  in Eqs. 8 and 9 generally converges rapidly. In Table 3 are listed the values of  $b_0$  obtained for several different combinations of the parameters involved, along with the number of cycles,  $N$ , required to compute the associated values of  $\zeta_0$  within a tolerance of 0.001. Note that convergence in all cases is achieved in one to three cycles.

#### ADJUSTED PROCEDURE

The data presented in the preceding section reveal that the accuracy of the linearization technique stems from the term representing the modified drag component of loading rather than the term representing the additional viscous damping. It would be reasonable, therefore, to expect that the reliability of this technique could be improved by retaining the added damping term in the form that has been presented but replacing the linearized drag force by the corresponding force for a non-interacting system (extreme right-hand member of Eq. 3).

When adjusted in this manner, the equivalent linearization technique is intimately related to, and under certain conditions reduces to, Penzien's decoupling technique examined in the next section.

## DECOUPLING TECHNIQUE GENERALIZED

Formulated originally for systems subjected to a wave loading only, the decoupling technique is generalized in this section for a wave acting in combination with a current of constant velocity,  $\dot{u}_c$ .

The equation of motion of the system in this case is given by

$$m\ddot{x} + c\dot{x} + kx = P_i \frac{\ddot{u}}{\ddot{u}_0} + P_d \frac{|\dot{v}-\dot{x}|(\dot{v}-\dot{x})}{\dot{u}_0^2} \quad (15)$$

in which  $x$  = the total displacement measured from the position of rest; and  $\dot{v}$ ,  $P_i$  and  $P_d$  are as previously defined. Recall that  $P_d$  represents the peak value of the drag component of the force due to the wave only, not the combination of wave and current.

On expanding the expression for the drag force, neglecting the term involving the square of  $\dot{x}$ , taking  $\text{sgn}(\dot{v}-\dot{x}) = \text{sgn}(\dot{v})$ , and transferring to the left member of the equation the term involving the product of  $\dot{v}$  and  $\dot{x}$ , one obtains

$$m\ddot{x} + (c + c'_0)\dot{x} + kx = P_i \frac{\ddot{u}}{\ddot{u}_0} + P_d \frac{|\dot{v}|\dot{v}}{\dot{u}_0^2} \quad (16)$$

in which  $c'_0$ , the viscous damping coefficient for the added damping approximating the effect of fluid-structure interaction, is a time-dependent quantity given by

$$c'_0 = [2 \text{sgn}(\dot{v}) \frac{\dot{v}}{\dot{u}_0}] \frac{P_d}{\dot{u}_0} \quad (17)$$

In his treatment of the effect of wave loading, Penzien [11] replaced the time-dependent product  $\dot{u} \text{sgn}(\dot{u})$  by the temporal mean of the absolute value of the fluid velocity,  $\langle |\dot{u}| \rangle$ . The use of the same approximation for the generalized fluid kinematics considered here leads to

$$c'_0 = 2 \frac{\langle |\dot{v}| \rangle}{\dot{u}_0} \frac{P_d}{\dot{u}_0} \quad (18)$$

When expressed in percent of the critical coefficient of damping,  $c_{cr}$ , the resulting hydrodynamic damping factor,  $\zeta_0$ , is given by

$$\zeta_0 = \frac{c'_0}{c_{cr}} = b'_0 \delta \quad (19)$$

in which

$$b'_0 = \frac{\langle |\dot{v}| \rangle}{\dot{u}_0} \quad (20)$$

and  $\delta$  is defined by Eq. 5. The factor  $b'_0$  is the counterpart of the factor  $b_0$  in the linearization technique.

For a normal random wave acting in combination with a current of constant velocity, it is a simple matter to show [10] that  $b'_0$  is given by

$$b'_0 = \sqrt{\frac{2}{\pi}} \frac{\sigma \dot{u}}{\dot{u}_0} \exp\left(\frac{-\dot{u}_c^2}{2\sigma \dot{u}}\right) + \frac{\dot{u}_c}{\dot{u}_0} \operatorname{erf}\left(\frac{\dot{u}_c}{\sqrt{2\sigma \dot{u}}}\right) \quad (21)$$

in which erf stands for the error function. For  $\dot{u}_c = 0$ , Eq. 21 reduces to the following expression presented in Ref. 11:

$$b'_0 = \sqrt{\frac{2}{\pi}} \frac{\sigma \dot{u}}{\dot{u}_0} \quad (22)$$

Equations 21 and the corresponding expression for  $\zeta_0$  are identical to those obtained by the equivalent linearization technique (Eq. 15 in Ref. 15) considering the structural velocity,  $\dot{x}$ , to be zero.

#### INTERRELATIONSHIP AND ACCURACY OF PROCEDURES

The interrelationship of the decoupling and linearization techniques may now be summarized as follows:

1. The drag component of loading in both the decoupling technique

and the adjusted version of the linearization technique is identical to that for a noninteracting system. By contrast, in the original linearization technique, it is a linear function of the fluid velocity.

2. Fluid-structure interaction increases the effective damping of the system and reduces the response. In the decoupling technique, the added damping is independent of the structural response and may be computed directly from the history of fluid particle velocity, whereas in the linearization techniques, it is also a function of the structural velocity and must be evaluated by iteration.

3. Provided that the added damping of the system in the linearization technique is determined assuming  $\dot{x} = 0$ , the adjusted version of this technique for a random normal wave acting in combination with a constant-velocity current is identical to the decoupling technique.

Representative response spectra computed by the decoupling technique are compared in Figs. 7 and 8 with the corresponding exact spectra. Fig. 7 refers to systems excited by the simulated wave loading only, whereas Fig. 8 also incorporates the effect of a current with  $\dot{u}_c = 0.5\dot{u}_0$ . Three different values of  $\alpha$  in the range between 0.5 and unity, and single values of  $\zeta$  and  $\delta$  are considered. No data are presented for values of  $\alpha$  less than 0.5 as the accuracy of the decoupling technique is quite high in this case.

Comparison of these data with the corresponding data presented in Figs. 5 and 6 reveals the following:

1. For systems with natural frequencies substantially higher than those for which the response spectra attain their absolute maximum values, the decoupling technique, and hence the adjusted linearization technique, are superior to the original version of the latter procedure. In the

spectral regions associated with the absolute maximum responses, the decoupling technique is inferior to the linearization technique but the differences are generally small in this case.

2. The decoupling technique generally underestimates the added damping and overestimates the maximum response. The errors increase with increasing  $\alpha$ , i.e., increasing contribution of the drag component of loading.

#### PROPOSED MODIFICATION OF DECOUPLING TECHNIQUE

**Effect of Load Factor,  $\alpha$ .** — It is desirable to examine at this stage the influence that this factor has on the characteristics of the exciting forces computed without regard for interaction. Representative histories for these forces are shown in Fig. 9 for several different values of  $\alpha$  in the range between zero and unity. The following trends should be observed:

1. Whereas the inertia force ( $\alpha = 0$ ) is characterized by oscillations of nearly equal peak values which are more or less uniformly distributed along the entire record, the major oscillations in the drag force ( $\alpha = 1$ ) are significantly fewer in number and generally widely separated. A consequence of the squaring of the velocity trace which tends to suppress the contributions of the smaller amplitude oscillations, the reduced repetitiveness of the drag force leads to a less severe resonant-like response and to reduced amplification factors for systems with natural frequencies close to the dominant frequency of the excitation than does the inertia force. This can clearly be seen from the response spectra for  $\alpha = 0$  and  $\alpha = 1$  compared in Fig. 10.

2. Because of the differences noted under item 1 and the fact that the peak ordinates of the inertia force component correspond to zero

ordinates of the drag force, the inertia force history generally dominates the characteristics of the total force and of the corresponding response spectra. For example, for  $\alpha = 0.5$  for which the peak values of the component forces are the same, the history of the combined force and the associated response spectrum are much closer to those of the inertia force than those of the drag force.

These observations suggest that, whereas for small values of  $\alpha$  the response of the system is influenced more or less uniformly by all pulses of the forcing function, for values of  $\alpha$  close to unity, it is dominated by the small number of pulses with the large amplitudes. It follows that the replacement of Eq. 17 by Eq. 18 would not be a good approximation for the larger values of  $\alpha$ , and that this approach would tend to underestimate the value of  $b'_0$  and the associated value of  $\tau_0$ .

Based on these considerations, it is recommended that for systems subjected to a purely drag component of loading, only those pulses in the fluid velocity history whose amplitudes exceed the 70 percent level of the absolute maximum velocity be considered in the averaging process. It is further recommended that the proposed threshold limit be considered to decrease linearly from the indicated value for  $\alpha = 1$  to zero for  $\alpha = 0$ . If  $z$  represents the appropriate limit in percent of the maximum fluid velocity, then  $z = 0.7\alpha$ .

This modification of the decoupling technique is tantamount to replacing the quantity  $\langle |\dot{v}| \rangle$  in Eq. 20 by  $\langle |\dot{v}_z| \rangle$ , the temporal mean of the absolute value of those pulses in the fluid velocity trace whose amplitudes exceed the specified threshold limit,  $z$ .

**Random Wave.** — For a normal random wave without any current, the

proposed approximation leads to the following expression (see Appendix I) for the factor  $b'_0$  in Eq. 19:

$$b'_0 = \frac{1 - F}{1 - z} \sqrt{\frac{2}{\pi}} \frac{\sigma \dot{u}}{\dot{u}_0} \quad (23)$$

in which  $F$  = the chi-square probability distribution function of three degrees of freedom, given by

$$F = \frac{1}{\sqrt{2\pi}} \int_0^s \sqrt{n} \exp(-\frac{n}{2}) dn \quad (24)$$

and  $s = 2 \ln[1/(1 - z)]$ . The values of  $F$  corresponding to different values of  $z = 0.7\alpha$  were computed by use of a standard IMSL subroutine [6], and the results led to the following linear approximation for  $b'_0$ :

$$b'_0 \approx [1 + 0.61\alpha] \sqrt{\frac{2}{\pi}} \frac{\sigma \dot{u}}{\dot{u}_0} \quad (25)$$

Note that for  $\alpha = 1$ , the values of  $b'_0$  and of the associated damping factor,  $\zeta'_0$ , are approximately 61 percent larger than those obtained from Penzien's original proposal. The difference in the two approaches naturally decreases with decreasing  $\alpha$ .

**Wave Combined with Current.** — For a sea state represented by a random wave in combination with a current, the exact expressions for  $b'_0$  are derived in Appendix I. Inasmuch as the evaluation of these expressions is tedious, the use of the following simpler approximation, obtained by modifying the first term of Eq. 21, is recommended instead:

$$b'_0 \approx (1 + 0.61\alpha) \sqrt{\frac{2}{\pi}} \frac{\sigma \dot{u}}{\dot{u}_0} \exp\left(\frac{-\dot{u}_c^2}{2\sigma \dot{u}}\right) + \frac{\dot{u}_c}{\dot{u}_0} \operatorname{erf}\left(\frac{\dot{u}_c}{\sqrt{2\sigma \dot{u}}}\right) \quad (26)$$

The values of  $b'_0$  determined from this approximation are plotted as a function of  $\dot{u}_c/\dot{u}_0$  in Fig. 11, where they are also compared with those

obtained from the corresponding exact expression.

**Accuracy of Procedure.** — The exact response spectra for the simulated sea state without any current considered previously are compared in Fig. 12 with those computed by the proposed modification of the decoupling technique. As before, the structural damping factor in these solutions is taken as  $\zeta = 0.02$ , and two different values of the loading factor,  $\alpha$ , and several values of the interaction parameter,  $\delta$ , are considered. The agreement between the two sets of results, excluding those corresponding to  $\alpha = 1$  and  $\delta = 0.5$ , is considered to be quite good. Comparable agreements have been obtained for several other sea states.

The results for  $\alpha = 1$  and  $\delta = 0.5$  correspond to an unrealistic combination of the parameters and should be viewed as an extreme test of the accuracy of the proposed approximation. Even in this case, however, this approximation is superior within the high frequency region of the response spectrum to those presented previously (see Fig. 13).

#### APPLICATION TO MORE COMPLEX SYSTEMS

The application of both the linearization and decoupling techniques to the analysis of multi-degree-of-freedom systems has already been described in the literature [4,8,11,12,14]. The proposed modification of the decoupling technique can be implemented in a similar manner, except that it is necessary to use for the damping coefficients,  $b'_0$ , the values corresponding to the fluid kinematics at the particular water depth under consideration.

The steps involved in the application of these techniques may be summarized as follows:

1. The wave and current forces exerted at various nodes of the struc-

ture are first computed from the fluid kinematics and the relevant tributary volumes and areas of the structure.

2. The drag components of these forces are then approximated in the manner indicated for single-degree-of-freedom systems, and two subsets of forces are obtained. The first, which is a function of the fluid particle velocities only, is retained on the right-hand member of the equations as modified drag forces, and the second, which is proportional to the structural velocities, is transferred to the left-hand member and interpreted as added damping forces.

3. The matrix for the overall damping of the system obtained in this manner has no relationship to either the mass or stiffness matrix of the system, and system damping is of the nonclassical type. To obviate the need for using complex-valued natural modes of vibration, the transformed modal damping matrix of the system is replaced by a diagonal matrix, the elements of which are determined by minimizing the square of the error between the damping forces associated with the original and the approximating matrices. Being functions of the response of the system, the elements of the diagonalized damping matrix must be computed by iteration.

4. With the overall damping of the system approximated in this manner, the analysis is implemented by use of the classical modal superposition method.

In the decoupling techniques, steps 1 through 4 are carried out only once, whereas in the linearization technique, they are repeated until the modal damping values corresponding to the starting and the derived sets of structural velocities agree within a prescribed tolerance.

**Proposed Simplification.** — While straightforward in principle, these procedures are generally time consuming and tedious. A simpler approximation for the modal damping values of the system may be obtained by deleting the off-diagonal terms of the transformed damping matrix referred to in item 4 of the preceding section. This approximation is presented in the following paragraphs for discrete, stick-like systems having a total of  $n$  submerged nodes.

Let  $P_{dj}$  be the maximum value of the drag component of the wave force acting on the  $j$ th node of the system, and  $\dot{u}_{0j}$  be the corresponding value of the wave-induced fluid particle velocity. Further, let  $\langle |\dot{v}_{zj}| \rangle$  be the relevant temporal mean of the absolute value of the total fluid velocity at that depth. (In the proposed modification of the decoupling technique, only those pulses with amplitudes in excess of the specified threshold limit,  $z = 0.7\alpha$ , are considered.) Finally, let

$$b'_{0j} = \frac{\langle |\dot{v}_{zj}| \rangle}{\dot{u}_{0j}} \quad (27)$$

$$\text{and } \delta_{ij} = \frac{\omega_i P_{dj}}{k_i^* \dot{u}_{0j}} \quad (28)$$

in which  $\omega_i$  = the  $i$ th circular natural frequency of vibration of the system;  $k_i^* = \omega_i^2 m_i^*$  = the generalized or effective stiffness of the  $i$ th natural mode; and  $m_i^*$  = the corresponding effective mass. For a normal random wave, the factors  $b'_{0j}$  may be determined from Fig. 11 or Eq. 26 using the values of  $\alpha$ ,  $\dot{u}_c/\dot{u}_0$  and  $\sigma_u$  that are appropriate to the particular node under consideration.

With these parameters and the approximation referred to, it is a simple matter to show that the percentage of the hydrodynamic damping

for the  $i$ th mode of vibration,  $\zeta_{oi}$ , is given by

$$\zeta_{oi} = \sum_{j=1}^n b'_{oj} \delta_{ij} \phi_{ij}^2 \quad (29)$$

in which  $\phi_{ij}$  = the ordinate at node  $j$  of the  $i$ th mode of vibration. If  $\zeta_i$  represents the corresponding percentage of structural damping, then the total damping factor for the  $i$ th mode of vibration,  $\tilde{\zeta}_i$ , is given by

$$\tilde{\zeta}_i = \zeta_i + \zeta_{oi} \quad (30)$$

Eqs. 29 and 30 are generalized versions of Eqs. 19 and 10, respectively.

The computation of the factors  $b'_{oj}$  and of the quantities  $P_{dj}$  and  $\dot{u}_{oj}$  in Eq. 28 still entails considerable effort, and an even simpler approximation for  $\zeta_{oi}$  is desirable. Considering that the response of the structure is dominated by the forces acting on its upper parts, it is recommended that the quantities  $P_{dj}$  and  $\dot{u}_{oj}$  in Eq. 28 be reinterpreted to be those corresponding to the instant,  $t_0$ , for which the drag component of the wave force at the uppermost, fully submerged node of the structure attains its maximum value. This node is typically located at a depth below mean water level approximately equal to the maximum surface wave height. It is further proposed that the factors  $b'_{oj}$  in Eq. 28 be replaced by a constant value,  $b'_0$ , determined from the fluid kinematics at the depth of the resultant of the drag forces at time  $t_0$ . This approximation has been tested for a number of structural systems and has been found to yield results of high accuracy.

As an indication of the differences in the values of  $\zeta_{oi}$  that may result from the use of the different approximations, in Table 4 are listed the results obtained for the first three modes of vibration of an offshore

guyed tower model in 1,600 ft. of water. The characteristics of the structure are given in Ref. 5. Its first three natural periods are 29.1 sec, 4.88 sec, and 2.33 sec, respectively. The results refer to a simulated sea state with the same surface wave characteristics as those considered previously and no current. Also listed in the table are the approximate and exact values of selected maximum responses.

As would be expected from the data presented in Fig. 5, the linearization technique for this highly compliant structure gives excellent results. However, this would not be the case for fixed-base structures which are associated with higher natural frequencies.

The proposed modification of the decoupling technique is clearly superior to the original version, and the simpler version of the proposed modification provides excellent approximations to the modal damping values. The latter values may be determined by this approach at a fraction of the time required by the linearization technique.

## CONCLUSION

With the information and concepts that have been presented, the effects of fluid-structure interaction on the maximum response of simple models of offshore structures can be estimated readily. The proposed approximation for the hydrodynamic modal damping factors of multi-degree-of-freedom systems should prove particularly useful in preliminary design decisions requiring an estimate of these quantities.

The equivalent linearization technique has been shown to lead to substantial errors for structures for which the drag component of the exciting force is dominant and for which the fundamental natural frequency of vibration is substantially higher than the dominant frequency of the

wave loading. Penzien's decoupling technique is superior in this case and the proposed modification further improves its accuracy.

#### **ACKNOWLEDGMENT**

This study was supported in part by the Minerals Management Service, U.S. Department of the Interior, and in part by Brown & Root International, Inc. and Rice University in Houston, Texas.

## APPENDIX I. — DERIVATION OF EQUATIONS

**Effects of Wave Only.**—For the normal random sea state considered, the probability density function of the wave amplitudes  $\dot{u}$  velocity trace of the fluid motion is a Rayleigh distribution, given by

$$p(\dot{u}) = \frac{\dot{u}}{\sigma_{\dot{u}}^2} \exp\left(\frac{-\dot{u}^2}{2\sigma_{\dot{u}}^2}\right) \quad (31)$$

If  $z$  represents a specified percentage of the absolute maximum velocity amplitude and  $\dot{u}_z$  represents the amplitude corresponding to that percentage, then the cumulative probability of the amplitudes with values greater than  $\dot{u}_z$  is given by

$$P(\dot{u} \geq \dot{u}_z) = \int_{\dot{u}_z}^{\infty} p(\dot{u}) d\dot{u} = 1 - z \quad (32)$$

On substituting Eq. 31 into Eq. 32, performing the indicated, integration, and taking the natural logarithms of the two members of the resulting expression, one obtains

$$\dot{u}_z = 2 \ln[1/(1-z)] \sigma_{\dot{u}} \quad (33)$$

Denoted by  $\langle |\dot{u}_z| \rangle$ , the temporal average of the velocity pulses with amplitudes in excess of  $\dot{u}_z$  is then given by

$$\langle |\dot{u}_z| \rangle = \frac{\int_{\dot{u}_z}^{\infty} \dot{u} p(\dot{u}) d\dot{u}}{\int_{\dot{u}_z}^{\infty} p(\dot{u}) d\dot{u}} = \frac{1}{1-z} \int_{\dot{u}_z}^{\infty} \frac{\dot{u}^2}{\sigma_{\dot{u}}^2} \exp\left(\frac{-\dot{u}^2}{2\sigma_{\dot{u}}^2}\right) d\dot{u} \quad (34)$$

which on integration yields

$$\langle |\dot{u}_z| \rangle = \frac{1-F}{1-z} \sqrt{\frac{2}{\pi}} \sigma_{\dot{u}} \quad (35)$$

The quantity  $F$  in this expression is defined by Eq. 24, in which  $n = \dot{u}^2 / \sigma_u^2$ . The ratio of  $\langle |\dot{u}_z| \rangle$  and  $\dot{u}_0$  represents the factor  $b'_0$  defined by Eq. 23.

**Effects of Combinations of Wave and Current.** — For a random sea state that includes a current with a constant velocity  $\dot{u}_c$ , the probability density function of the peaks of the total velocity trace,  $\dot{v} = \dot{u}_c + \dot{u}$ , is given by [10]

$$p(\dot{v}) = \frac{\dot{v}}{\sigma_u^2} I_0\left(\frac{\dot{u}_c \dot{v}}{\sigma_u^2}\right) \exp\left(-\frac{\dot{v}^2 + \dot{u}_c^2}{2\sigma_u^2}\right) \quad (36)$$

Proceeding as in the preceding section, the following relationship is obtained between the specified percentage of the absolute maximum value of the total velocity trace,  $z$ , and the corresponding total velocity amplitude,  $\dot{v}_z$ :

$$1 - z = \int_{\dot{v}_z}^{\infty} \frac{\dot{v}}{\sigma_u^2} I_0\left(\frac{\dot{u}_c \dot{v}}{\sigma_u^2}\right) \exp\left(-\frac{\dot{v}^2 + \dot{u}_c^2}{2\sigma_u^2}\right) d\dot{v} \quad (37)$$

which on introducing the parameter  $\theta = \dot{v}^2 / (2\sigma_u^2)$  and properly adjusting the lower limit of integration can also be written as

$$1 - z = \exp\left(\frac{-\dot{u}_c^2}{2\sigma_u^2}\right) \int_{\dot{v}_z^2 / 2\sigma_u^2}^{\infty} I_0\left(\frac{\sqrt{2} \dot{u}_c}{\sigma_u} \sqrt{\theta}\right) \exp(-\theta) d\theta \quad (38)$$

Unlike the corresponding expression in the preceding section from which a closed-form expression could be obtained for  $\dot{v}_z$  by formal integration, in the present case this does not appear to be possible, and the value of  $\dot{v}_z$  corresponding to a specified  $z$  must be computed iteratively

by numerical integration. A first approximation to  $\dot{v}_z$  may be determined from

$$\dot{v}_z = 2 \ln[1/(1-z)] \sigma_{\dot{u}} + \dot{u}_c \quad (39)$$

Let  $\langle |\dot{v}_z| \rangle$  represent the temporal average of the velocity pulses with amplitudes  $\dot{v}$  in excess of  $\dot{v}_z$ . When measured from the level of the current velocity,  $\dot{u}_c$ , the amplitudes of the velocity pulses have a Rayleigh distribution. Accordingly, the value of  $\langle |\dot{v}_z| \rangle$  may be determined from the right hand member of Eq. 34 noting that  $\dot{u}_z = \dot{v}_z - \dot{u}_c$ , and interpreting the quantity  $(2/\pi)\dot{u}$  in this equation as the temporal average of the absolute value of a velocity pulse of amplitude  $\dot{u}$  that is superimposed on the current velocity,  $\dot{u}_c$ . Denoted by  $\dot{w}$ , the latter quantity is given by

$$\dot{w} = \frac{1}{2\pi} \int_0^{2\pi} |\dot{u}_c + \dot{u} \sin \tau| d\tau \quad (40)$$

in which  $\tau$  denotes time. Integration of Eq. 40 yields

$$\dot{w} = \begin{cases} \dot{u}_c & \text{for } \dot{u} \leq \dot{u}_c \\ \sqrt{\frac{2}{\pi}} \dot{u} \left[ \frac{\dot{u}_c}{\dot{u}} \sin^{-1} \left( \frac{\dot{u}_c}{\dot{u}} \right) + \sqrt{1 - \left( \frac{\dot{u}_c}{\dot{u}} \right)^2} \right] & \text{for } \dot{u} > \dot{u}_c \end{cases} \quad (41)$$

On substituting Eq. 41 in the reinterpreted version of Eq. 34 and evaluating the integrals involved, one obtains

$$\langle |\dot{v}_z| \rangle = \exp\left(\frac{\dot{u}_z^2}{2\sigma_{\dot{u}}^2}\right) \left\{ \sqrt{\frac{2}{\pi}} \sigma_{\dot{u}} \exp\left(\frac{-\dot{u}_c^2}{2\sigma_{\dot{u}}^2}\right) + \dot{u}_c \left[ 1 + \operatorname{erf}\left(\frac{\dot{u}_c}{\sqrt{2}\sigma_{\dot{u}}}\right) \right] \right\} - \dot{u}_c$$

$$\text{for } \dot{v}_z \leq 2\dot{u}_c \quad (42)$$

and

$$\begin{aligned}
 \langle |\dot{v}_z| \rangle = & \frac{2}{\pi} \left[ \dot{u}_c \sin^{-1} \left( \frac{\dot{u}_c}{\dot{u}_z} \right) + \dot{u}_z \sqrt{1 - \left( \frac{\dot{u}_c}{\dot{u}_z} \right)^2} \right] \\
 & + \exp \left( \frac{\dot{u}_z^2}{2\sigma_u^2} \right) \left\{ \sqrt{\frac{2}{\pi}} \sigma_u \exp \left( \frac{-\dot{u}_c^2}{2\sigma_u^2} \right) - \dot{u}_c \left[ 1 - \operatorname{erf} \left( \frac{\dot{u}_c}{\sqrt{2} \sigma_u} \right) \right] \right. \\
 & \left. - \frac{2}{\pi} \int_{\dot{u}_c}^{\dot{u}_z} \sqrt{\frac{\dot{u}^2 - \dot{u}_c^2}{\dot{u}}} \exp \left( \frac{-\dot{u}^2}{2\sigma_u^2} \right) d\dot{u} \right\} \text{ for } \dot{v}_z > 2\dot{u}_c \quad (43)
 \end{aligned}$$

The factor  $b_0'$  is defined by the ratio of  $\langle |\dot{v}_z| \rangle$  and  $\dot{u}_0$ . For  $\dot{u}_c = 0$ , Eq. 43 reduces as it should to Eq. 35.

## APPENDIX II. - REFERENCES

1. Abromowitz, M., and Stegun, I.A., Handbook of Mathematical Functions, Dover Publications, Inc., New York, NY, 1970, pp. 504.
2. Borgman, L.E., "Spectral Analysis of Ocean Wave Forces on Piling," Journal of Waterways and Harbors Division, ASCE, Vol. 93, No. WW2, May, 1967, pp. 129-156.
3. Dao, B.V., and Penzien, J., "Comparison of Treatments of Non-linear Drag Forces Acting on Fixed Offshore Platforms," Applied Ocean Research, 1982, Vol. 4, No. 2, pp. 66-72.
4. Foster, E. T., "Model for Nonlinear Dynamics of Offshore Towers," Journal of Engineering Mechanics Division, ASCE, Vol. 96, No. EM1, Feb., 1970, pp. 41-66.
5. Hahn, G., and Veletsos, A. S., "Dynamic Response of Offshore Guyed Towers," Structural Research at Rice, Report No. 33, Department of Civil Engineering, Rice University, Houston, TX, August, 1985.
6. International Mathematical and Statistical Libraries, Subroutine MDCH, IMSL Inc., Houston, TX, June, 1982.
7. Laya, E.J., Connor, J.J., and Shyam Sunder, S., "Hydrodynamic Forces on Flexible Offshore Structures," Journal of Engineering Mechanics Division, ASCE, Vol. 110, No. 3, Mar., 1984, pp. 433-448.
8. Malhotra, A.K., and Penzien, J., "Nondeterministic Analysis of Offshore Structures," Journal of Engineering Mechanics Division, ASCE, Vol. 96, No. EM6, Dec., 1970, pp. 985-1003.
9. Nagashima, E., "Dynamic Response of a Vertical Cylinder due to Wave Forces," Master's Thesis submitted to the University of Texas at Austin, Texas, (directed by J.M. Roesset), May, 1981.
10. Papoulis, A., Probability, Random Variables and Stochastic Processes, McGraw-Hill, First Edition, 1965, pp. 121 and 139.
11. Penzien, J., "Structural Dynamics of Fixed Offshore Structures," BOSS'76, Proceedings of International Conference on the Behavior of Offshore Structures, Vol. 1, Trondheim, Norway, Aug. 1976, pp. 581-592.
12. Penzien, J., and Tseng, S., "Three-Dimensional Dynamic Analysis of Fixed Offshore Platforms," Numerical Methods in Offshore Engineering, O.C. Zienkiewicz, Ed., John Wiley and Sons, New York, NY, 1978, pp. 221-243.
13. Sarpkaya, T., and Isaacson, M., Mechanics of Wave Forces on Offshore Structures, Von Nostrand Reinhold, New York, NY, 1981.
14. Shyam Sunder, S., and Connor, J.J., "Sensitivity Analyses for Steel Jacket Offshore Platforms," Dynamic Analysis of Offshore Structures, C. L. Kirk, Ed., Gulf Publishing Company, Houston, TX, pp. 11-24.
15. Spanos, P-T. D., and Chen, T.W., "Random Response to Flow Induced Forces," Journal of Engineering Mechanics Division, ASCE, Vol. 107, No. EM6, Dec., 1981, pp. 1173-1190.

### APPENDIX III.— NOTATION

The following symbols are used in this paper:

- $b_0$  = constant in expression for the hydrodynamic damping determined by equivalent linearization technique;
- $b_0^i$  = constant in expression for the hydrodynamic damping determined by the decoupling techniques;
- $b_{0j}^i$  = value of  $b_0^i$  at  $j$ th submerged node;
- $c$  = coefficient of viscous structural damping coefficient;
- $c_0, c_0^i$  = coefficients of added damping due to effect of fluid-structure interaction;
- $F$  = chi-square probability function with three degrees of freedom;
- $f$  = natural frequency of the structure, in cps;
- $k$  = structural stiffness;
- $k_i^*$  = generalized structural stiffness for the  $i$ th natural mode of vibration;
- $m$  = total mass of structure, including added mass due to hydrodynamic inertia effect;
- $m_i^*$  = generalized total mass for the  $i$ th natural mode of vibration;
- $P$  = maximum value of total hydrodynamic force due to wave only;
- $P_d$  = maximum value of drag component of hydrodynamic force due to wave only;
- $P_{dj}$  = value of  $P_d$  for  $j$ th submerged node;
- $P_i$  = maximum value of inertia component of hydrodynamic force due to wave only;
- $\dot{u}$  = fluid particle velocity due to wave only;
- $\dot{u}_c$  = velocity of current;
- $\dot{u}_0$  = absolute maximum value of  $\dot{u}$ ;
- $\dot{u}_{0j}$  = value of  $\dot{u}_0$  for  $j$ th submerged node;
- $\dot{u}$  = threshold amplitude of fluid velocity used in computation of  $b_0^i$ .
- $\dot{v}$  =  $\dot{u} + \dot{u}_c$  = total fluid particle velocity due to wave and current;
- $\dot{v}_z$  = threshold amplitude of total fluid velocity used in computation of  $b_0^i$ ;

- $\dot{v}_{zj}$  = value of  $\dot{v}_z$  for  $j$ th submerged node;
- $x$  = structural displacement, measured from undeflected position of structures;
- $x_0$  = temporal mean of the displacement of the structure due to combination of the wave and current loadings;
- $x_{st}$  = static displacement of structure due to the peak value of the total hydrodynamic force induced by the wave component of loading;
- $(x_{st})_d$  = static displacement due to the peak value of the drag force induced by the wave component of loading;
- $z$  = threshold percentage of velocity amplitudes considered in computation of the temporal average of fluid particle velocity;
- $\alpha$  = dimensionless load factor defining the relative magnitudes of the drag and inertia components of the hydrodynamic forces due to wave only;
- $\delta$  = dimensionless fluid-structure interaction parameter defined by Eq. 5;
- $\delta_{ij}$  = dimensionless fluid-structure interaction parameter for  $j$ th submerged node of a system vibrating in  $i$ th natural mode; given by Eq. 28;
- $\Delta P(t)$  = difference in effective exciting forces for interacting and non-interacting systems subjected to a wave loading only;
- $\Delta x(t)$  = difference in displacements of interacting and non-interacting systems subjected to wave loading only;
- $\{\phi_j\}$  =  $i$ th modal vector;
- $\zeta$  = structural damping factor, in percent of critical damping;
- $\bar{\zeta}$  =  $\zeta + \zeta_0$  = total system, in percent of critical damping;
- $\bar{\zeta}_i$  = value of  $\bar{\zeta}$  for  $i$ th mode of vibration;
- $\zeta_0$  = added damping factor in percent of critical damping, approximating effects of fluid-structure interaction;
- $\zeta_{0i}$  = value of  $\zeta_0$  for  $i$ th mode of vibration;
- $\sigma_u$  = standard deviation of fluid particle velocity due to wave only;
- $\omega$  = circular natural frequency of simple oscillator;
- $\omega_j$  =  $i$ th circular natural frequency of system.

TABLE 1. — Peak Values of Exciting Force and Resulting Response for Systems without and with Interaction

f cps	$\alpha = 1.0$		$\alpha = 0.75$		$\alpha = 0.50$		$\alpha = 0.25$	
	$\delta = 0$	$\delta = 0.10$	$\delta = 0$	$\delta = 0.10$	$\delta = 0$	$\delta = 0.10$	$\delta = 0$	$\delta = 0.10$
Values of $ P_{\max} /P$								
0.04	1.000	0.943	1.000	0.913	1.000	0.912	1.000	0.979
0.08		0.720		0.694		0.775		0.929
0.10		0.783		0.816		0.815		0.954
0.20		0.941		1.008		1.068		0.978
0.333		0.960		0.939		1.004		1.006
0.50		1.012		1.012		0.984		1.004
Values of $ x_{\max} /x_{st}$								
0.04	0.809	0.691	0.851	0.712	0.929	0.740	0.862	0.691
0.08	3.452	2.212	3.744	2.526	4.705	3.237	5.004	3.118
0.10	2.499	1.856	2.358	1.976	3.389	2.560	4.340	2.762
0.20	1.628	1.202	1.306	1.038	1.352	1.618	1.530	1.735
0.333	1.537	1.363	1.417	1.271	1.064	1.074	1.199	1.219
0.50	1.127	1.085	1.177	1.133	1.135	1.107	1.050	1.061

TABLE 2.— Comparison of Maximum Values of Forces for Systems without Interaction Computed Exactly and by the Linearization Technique

Value of $\alpha$	Values of $ P_{\max} /(P_i + P_d)$					
	$\dot{u}_c/\dot{u}_0 = 0$		$\dot{u}_c/\dot{u}_0 = 0.5$		$\dot{u}_c/\dot{u}_0 = 1.0$	
	Exact	Linearized	Exact	Linearized	Exact	Linearized
(1)	(2)	(3)	(4)	(5)	(6)	(7)
1	1.000	0.532	2.250	1.420	4.000	3.154
0.75	0.773	0.481	1.702	1.108	3.011	2.388
0.50	0.645	0.595	1.218	0.938	2.068	1.710
0.25	0.768	0.785	0.948	0.924	1.301	1.232
0	1	1	1	1	1	1

TABLE 3.— Convergence of Values  $b_o$  in Equivalent Linearization Technique

f cps	$\dot{u}_c/\dot{u}_o = 0$		$\dot{u}_c/\dot{u}_o = 0.5$		$\dot{u}_c/\dot{u}_o = 1.0$	
	$b_o$	N	$b_o$	N	$b_o$	N
$\alpha = 1$						
0.04	0.266	1	0.524	1	0.999	2
0.10	0.255	2	0.524	1	1.015	1
0.25	0.266	1	0.524	1	1.015	1
0.50	0.266	1	0.524	1	1.015	1
$\alpha = 0.75$						
0.04	0.254	2	0.512	2	0.999	2
0.10	0.266	1	0.524	1	1.004	2
0.20	0.266	1	0.524	1	1.015	1
0.50	0.266	1	0.524	1	1.015	1
$\alpha = 0.50$						
0.04	0.240	2	0.509	2	1.000	2
0.10	0.300	2	0.524	1	0.999	2
0.20	0.283	2	0.536	2	1.026	2
0.50	0.266	1	0.524	1	1.015	1
$\alpha = 0.25$						
0.04	0.204	2	0.502	2	1.015	1
0.10	0.408	3	0.575	2	0.995	2
0.20	0.323	2	0.562	2	1.040	2
0.50	0.266	1	0.524	1	1.015	1

TABLE 4. — Comparison of Solutions for a Guyed-Tower Model in 1600 ft. of Water

Exact	Linearization Technique	Penzien's Decoupling	Modified Decoupling	
			Refined	Simple
Hydrodynamic Modal Damping Factor, $\zeta_{oi}$ , for $i = 1, 2,$ and $3,$ respectively				
---	0.133	0.174	0.242	0.235
---	0.022	0.007	0.015	0.014
---	0.012	0.003	0.006	0.005
Maximum Top Displacement, in ft.				
14.38	14.62	17.25	15.70	15.85
Maximum Base Shear, in kips				
3,840	3,726	4,481	3,879	3,890
Maximum Base Moment, in kip-ft. $\times 10^{-6}$				
0.233	0.243	0.286	0.256	0.259
Maximum Moment at 520 ft. Depth, in kip-ft. $\times 10^{-6}$				
1.833	1.772	2.038	1.936	1.943

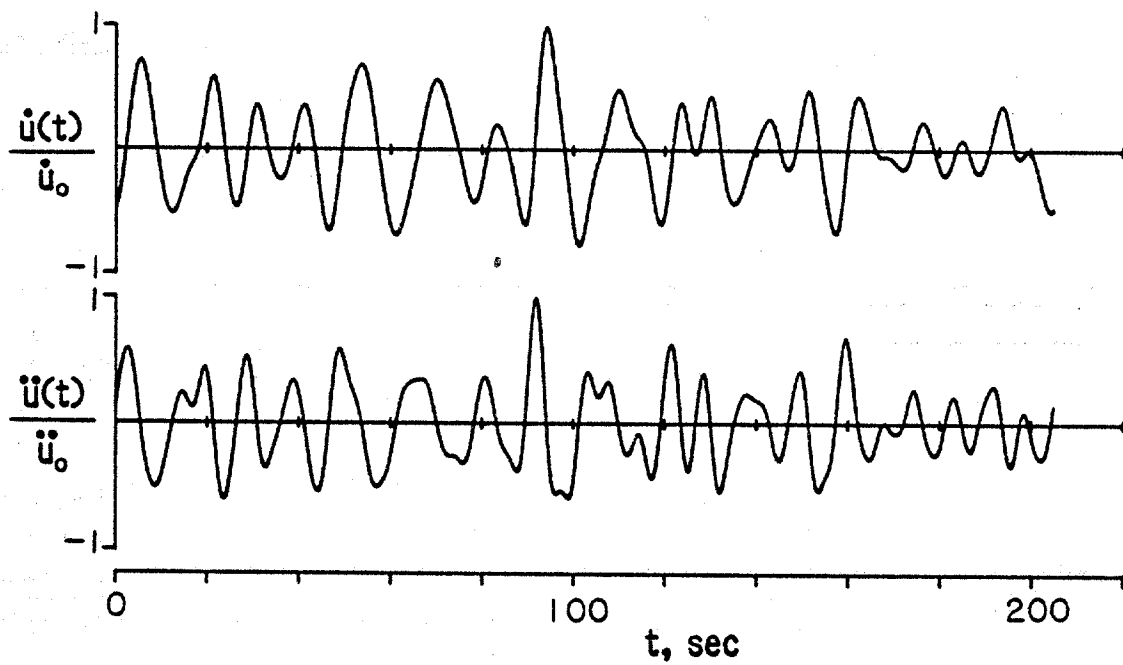


FIG. 1. Normalized Fluid Kinematics

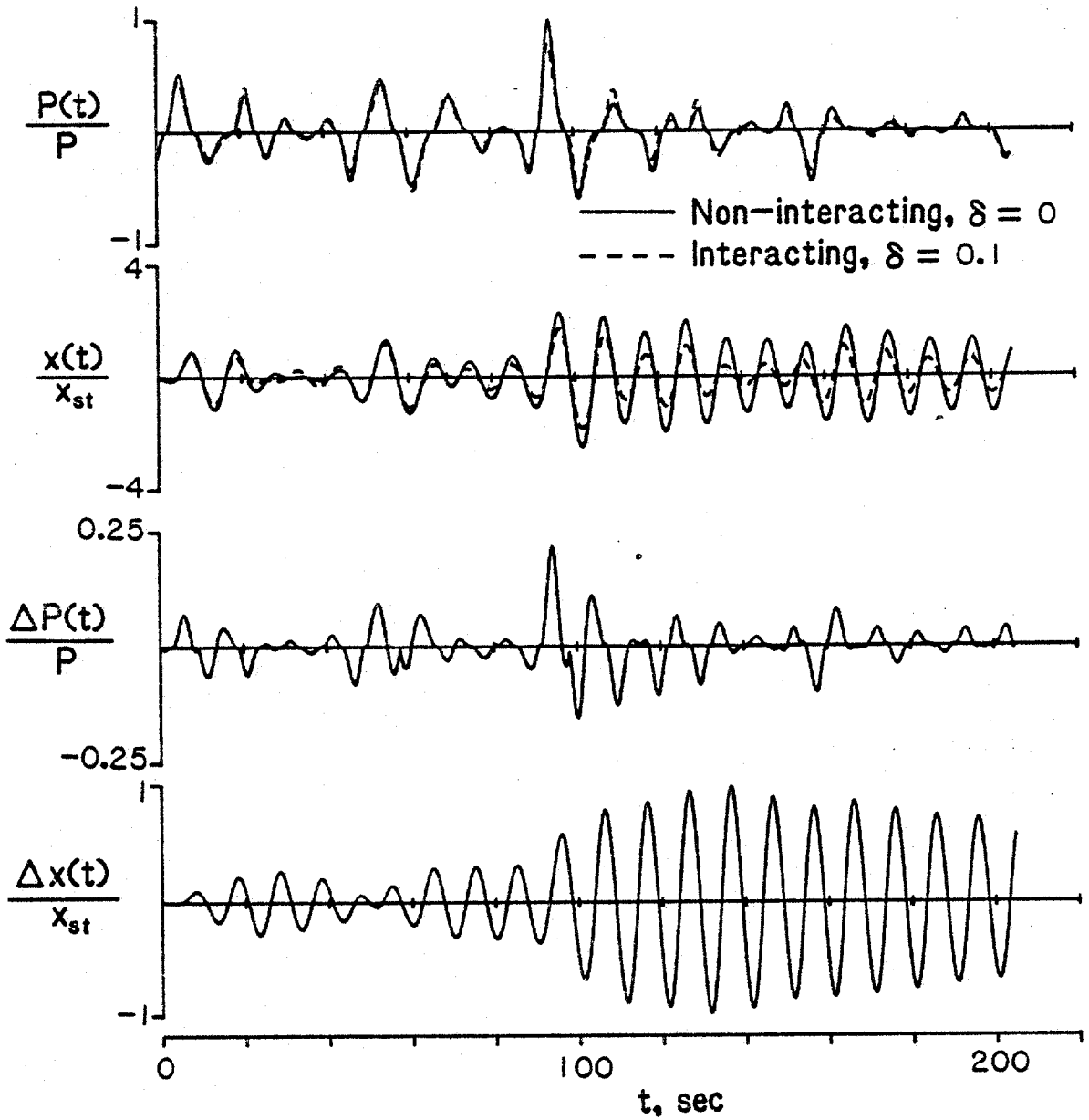


FIG. 2. Normalized Histories of Forces and Displacements for Systems with  $\zeta = 0.02$  and  $f = 0.1$  cps

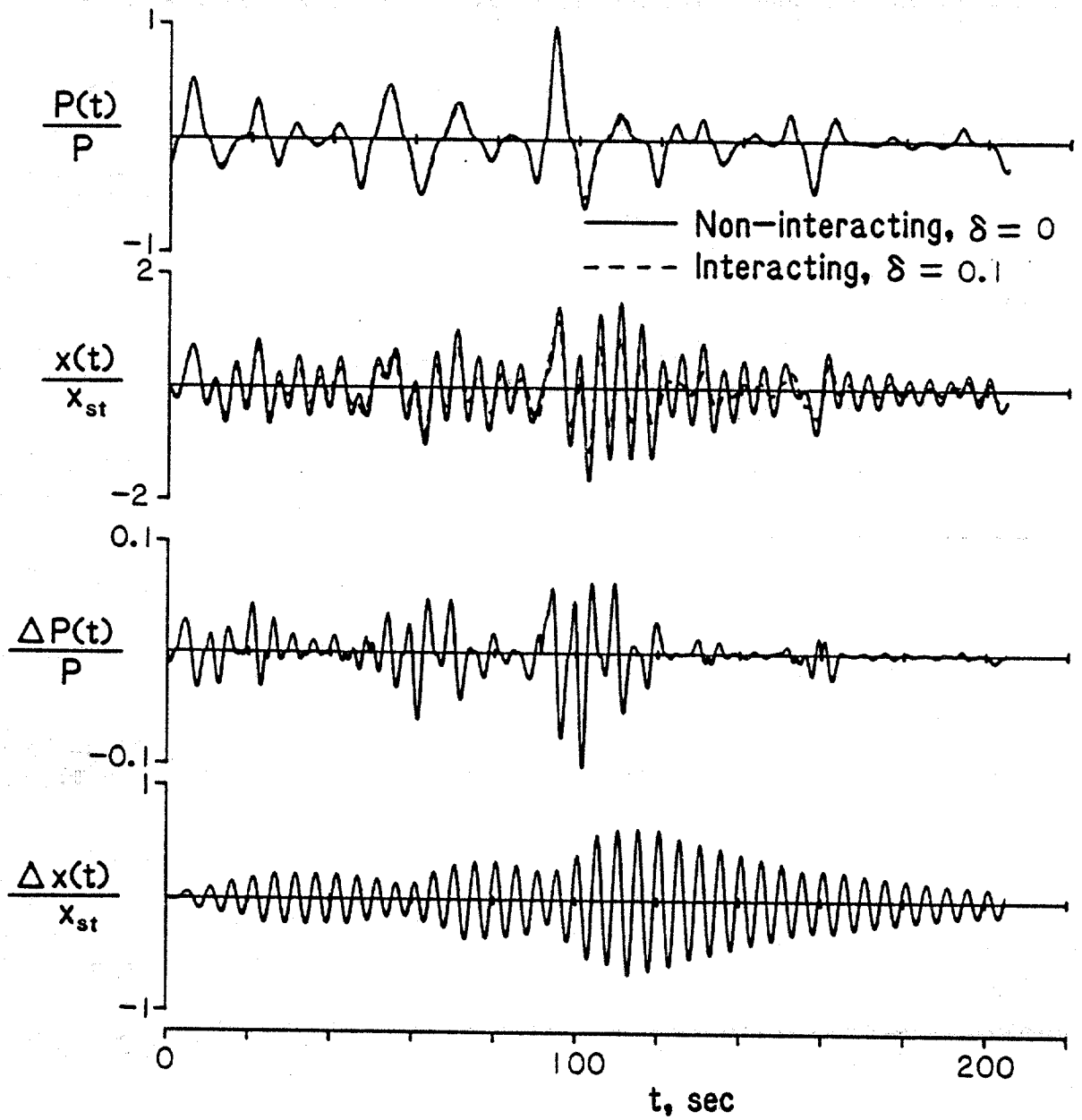


FIG. 3. Normalized Histories of Forces and Displacements for Systems with  $\zeta = 0.02$  and  $f = 0.2$  cps

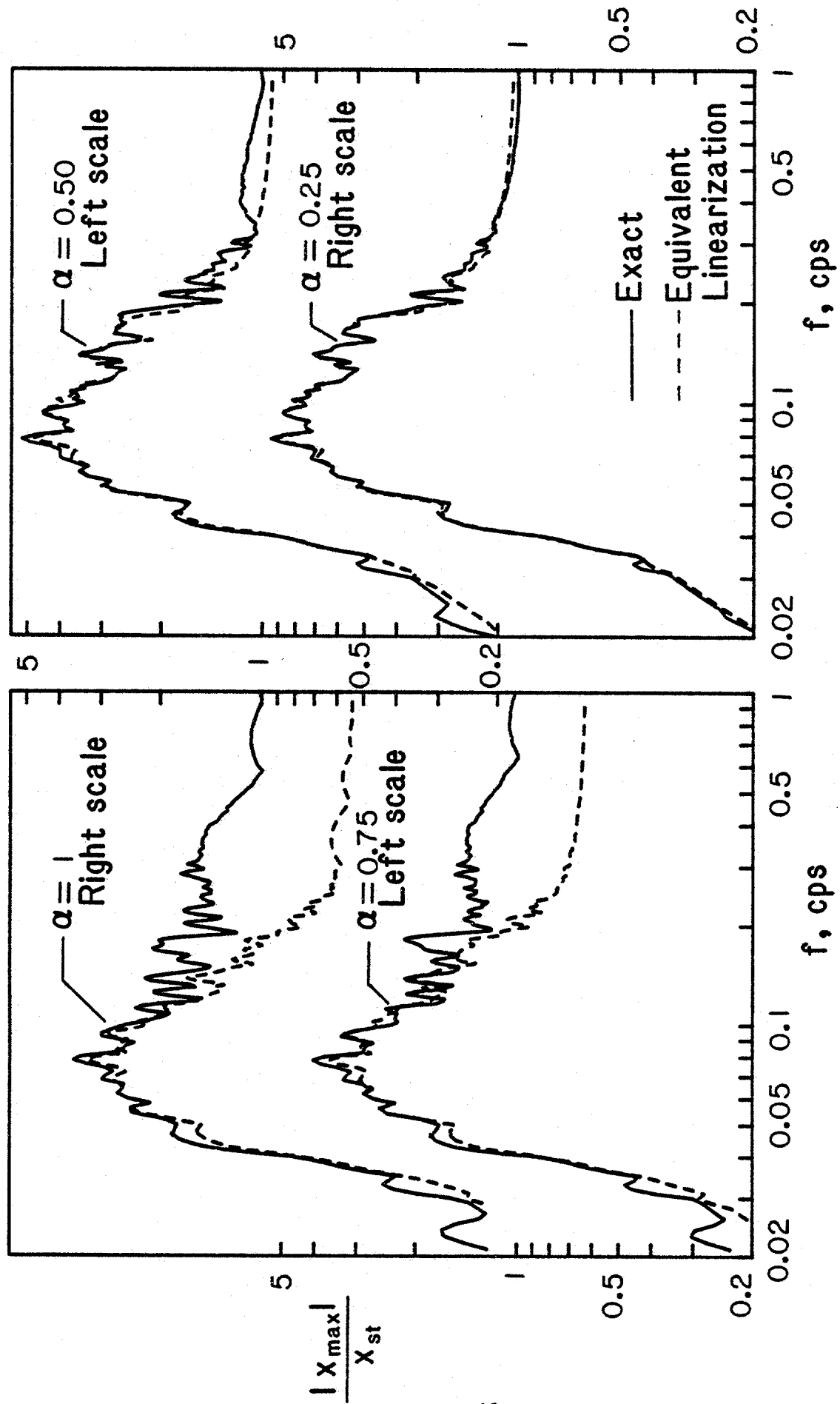


FIG. 4. Response Spectra for Non-Interacting Systems with  $\zeta = 0.02$  Subjected to Wave Loading

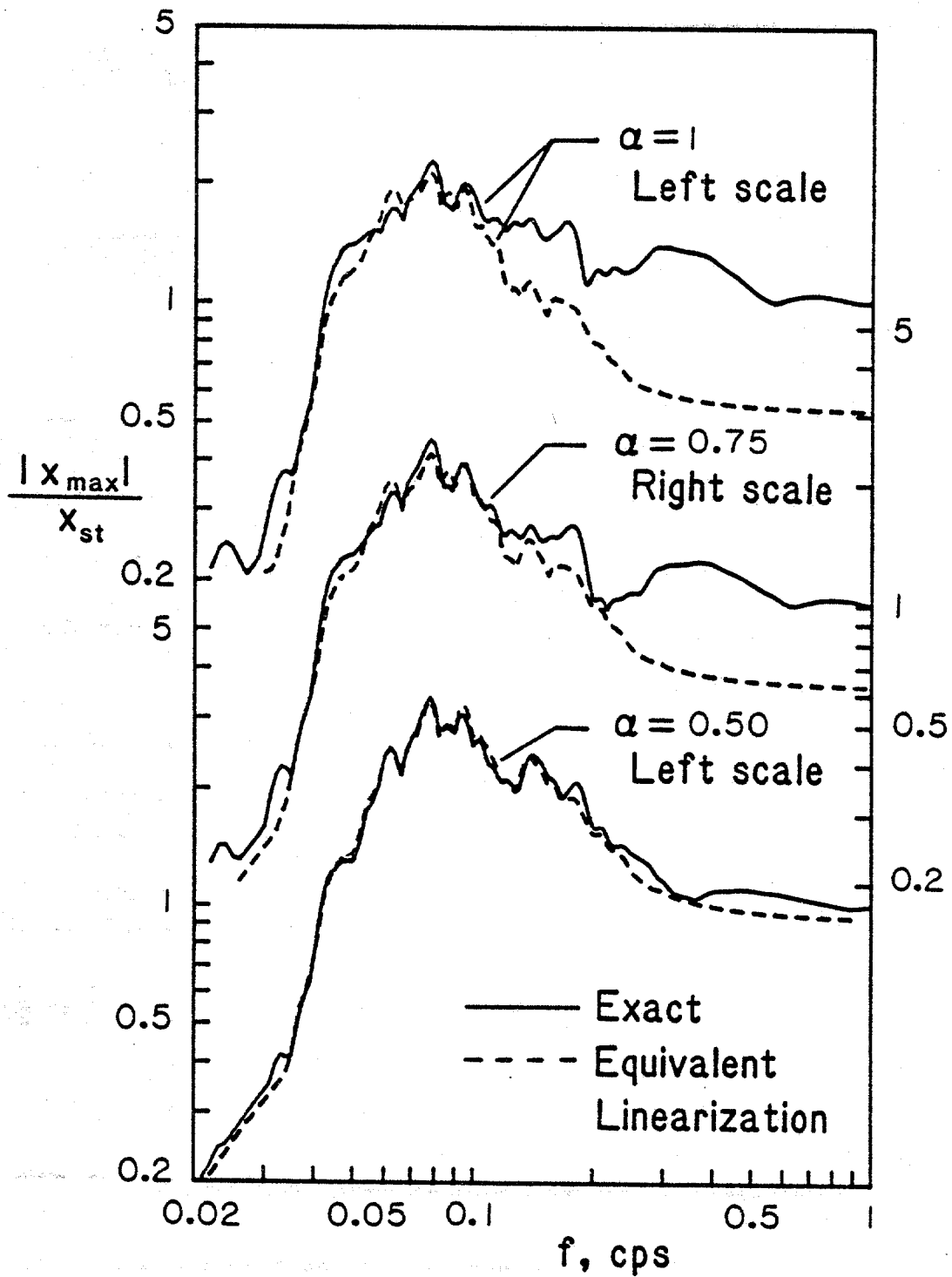


FIG. 5. Response Spectra for Interacting Systems with  $\delta = 0.10$  and  $\zeta = 0.02$  Subjected to Wave Loading

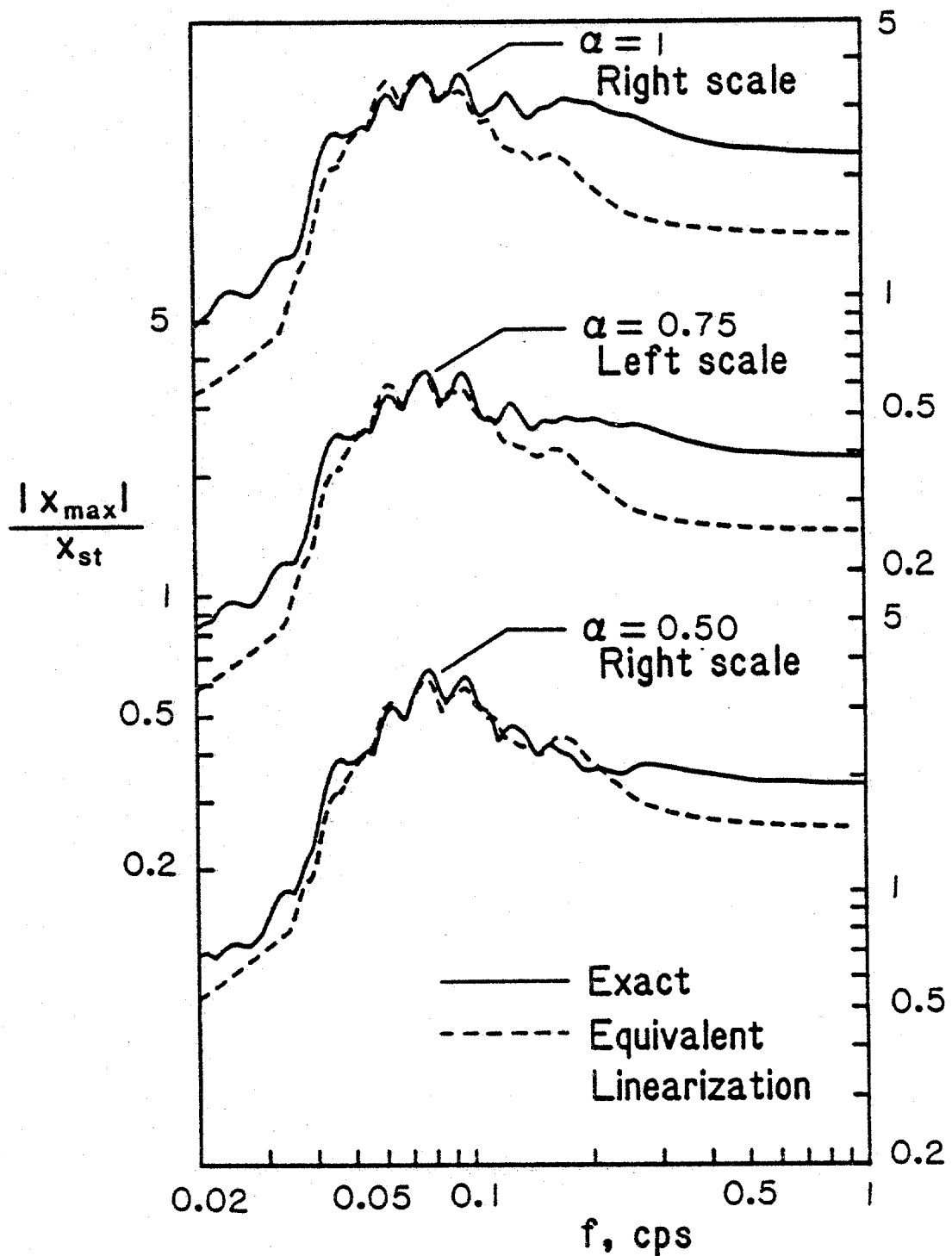


FIG. 6. Response Spectra for Interacting Systems with  $\delta = 0.10$  and  $\zeta = 0.02$  Subjected to Combination of Wave and Current with  $u_c = 0.5u_0$

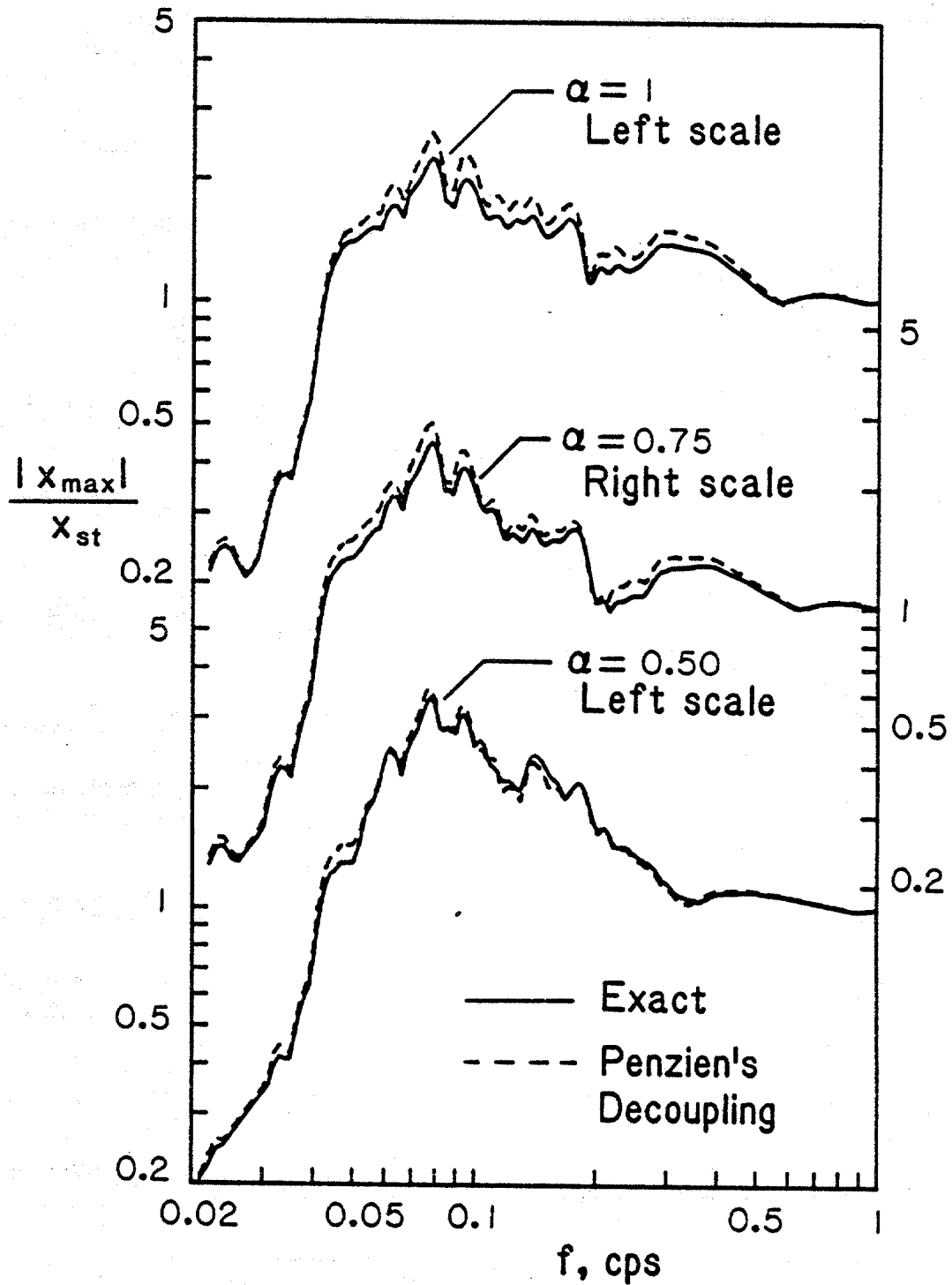


FIG. 7. Comparison of Response Spectra Obtained by Exact Method and by Decoupling Technique; Systems with  $\delta = 0.10$  and  $\zeta = 0.02$  Subjected to Wave Only

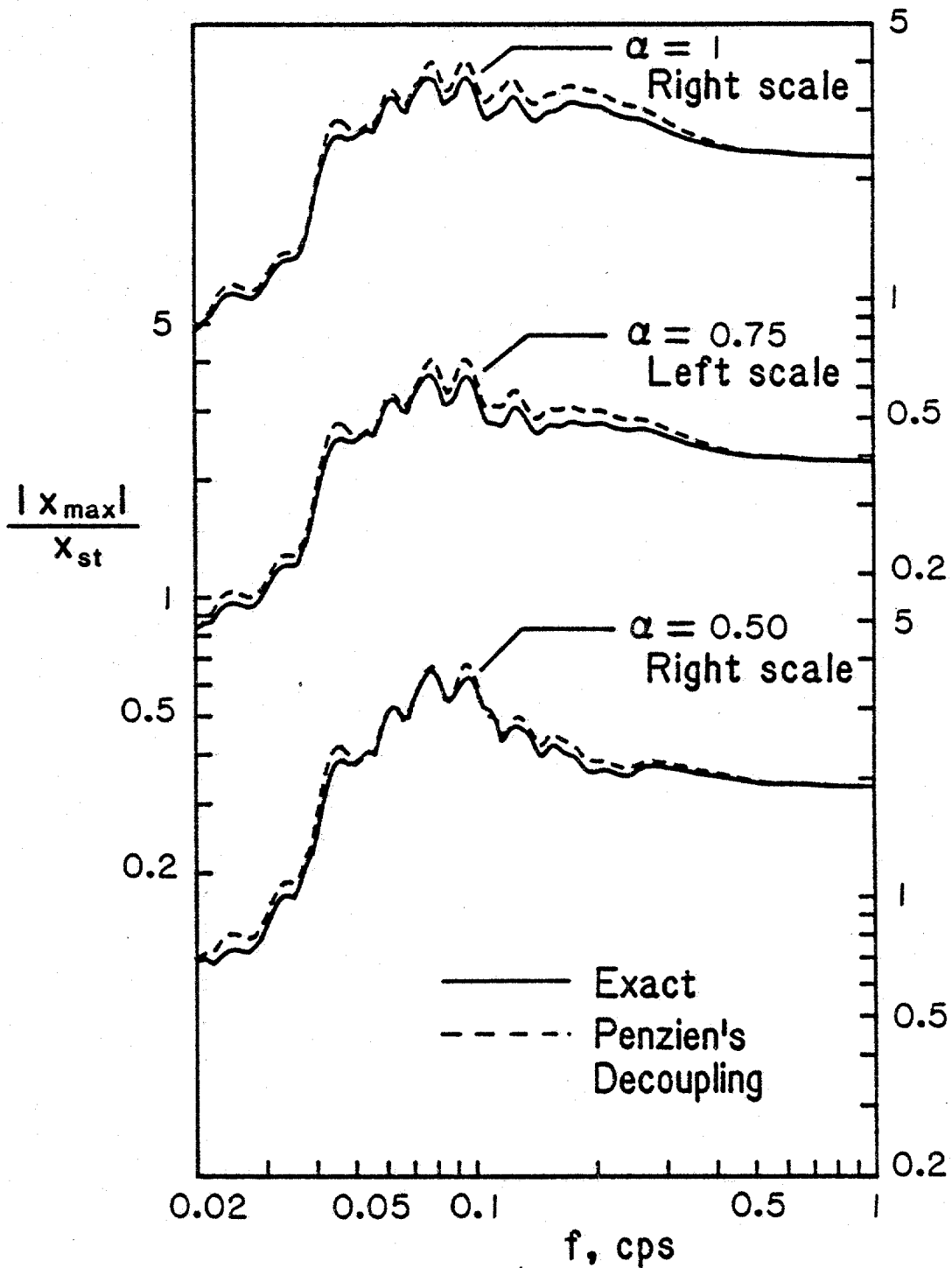


FIG. 8. Comparison of Response Spectra Obtained by Exact Method and by Decoupling Technique; Systems with  $\delta = 0.10$  and  $\zeta_s = 0.02$  Subjected to Wave and Current with  $\dot{u}_c = 0.5 \dot{u}_0$

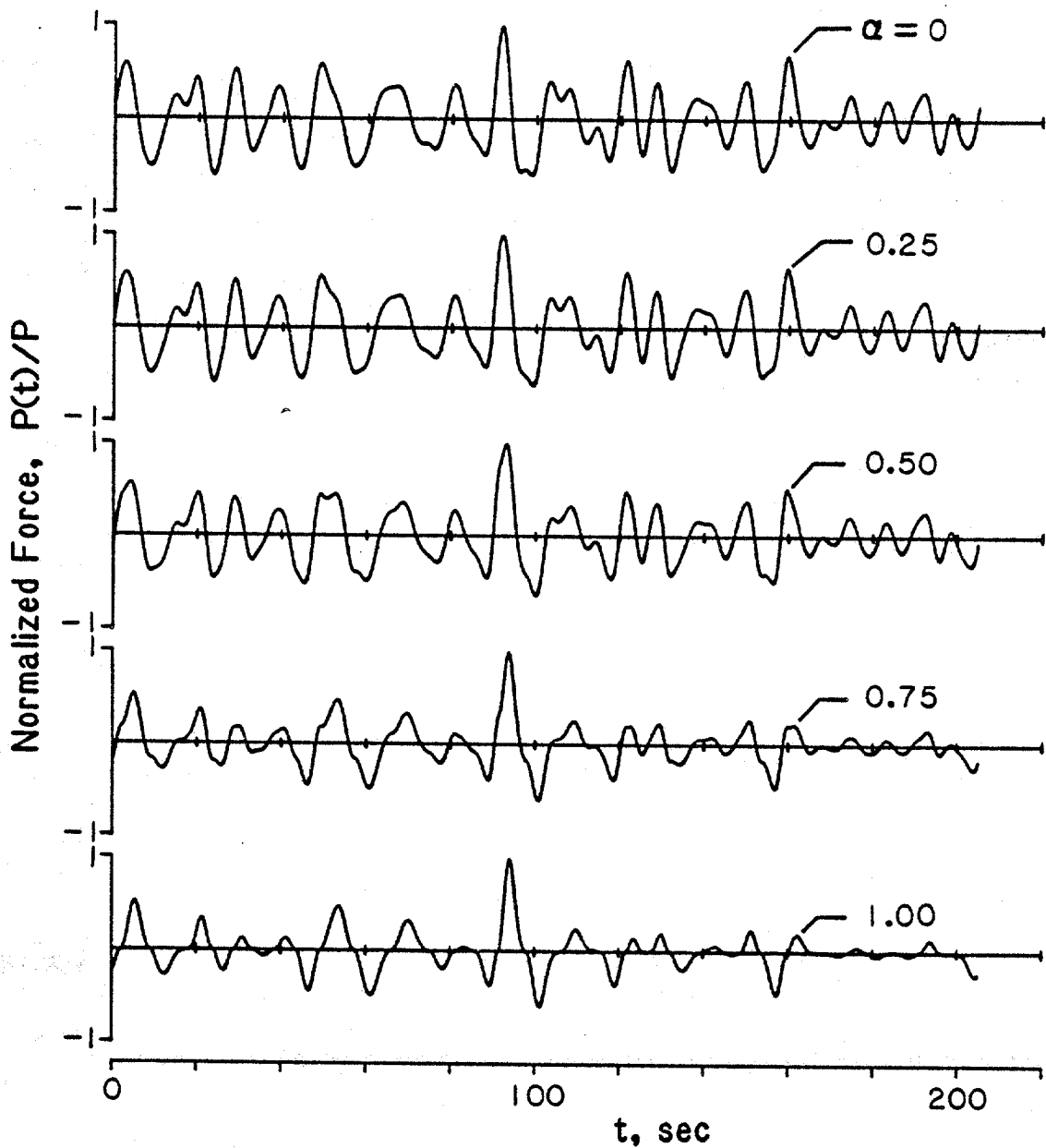


FIG. 9. Effect of Load Factor,  $\alpha$ , on Histories of Exciting Forces for Systems without Interaction

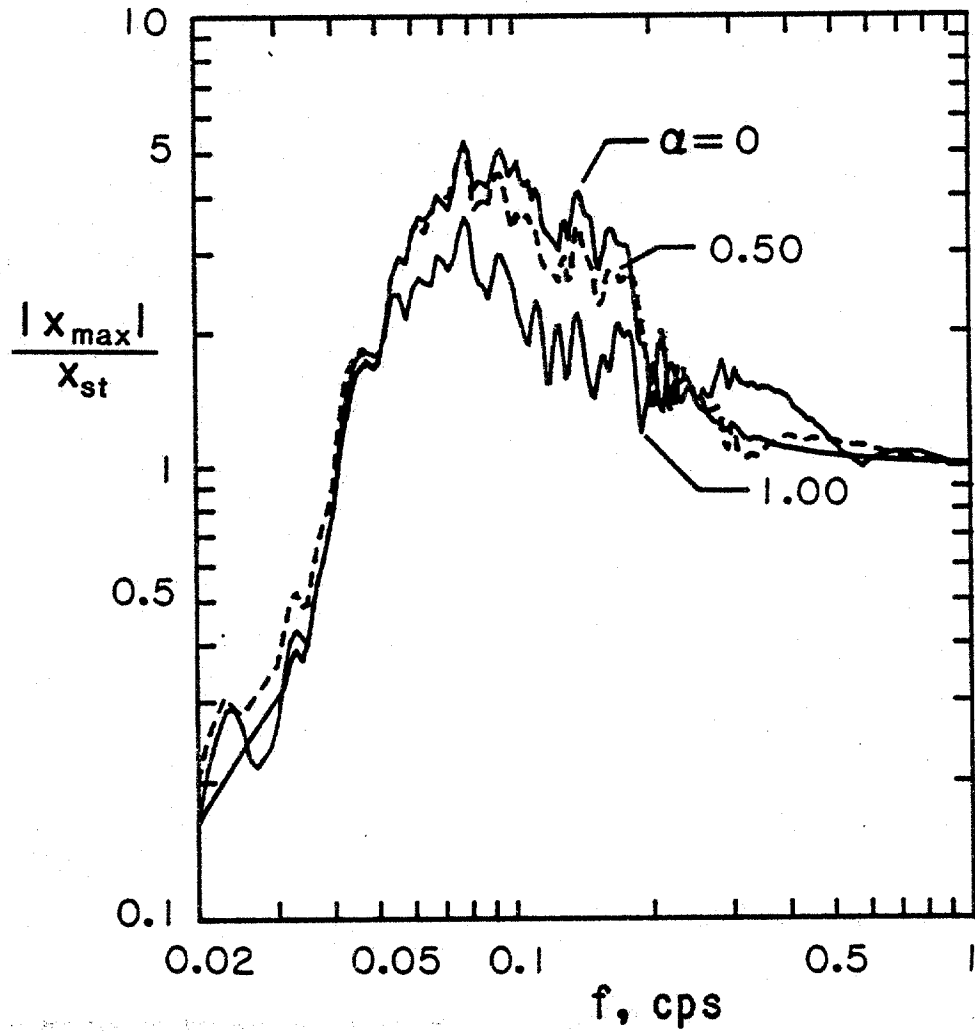


FIG. 10. Effect of Load Factor,  $\alpha$ , on Characteristics of Response Spectra for Non-Interacting Systems with  $\zeta = 0.02$  Subjected to Wave Loading

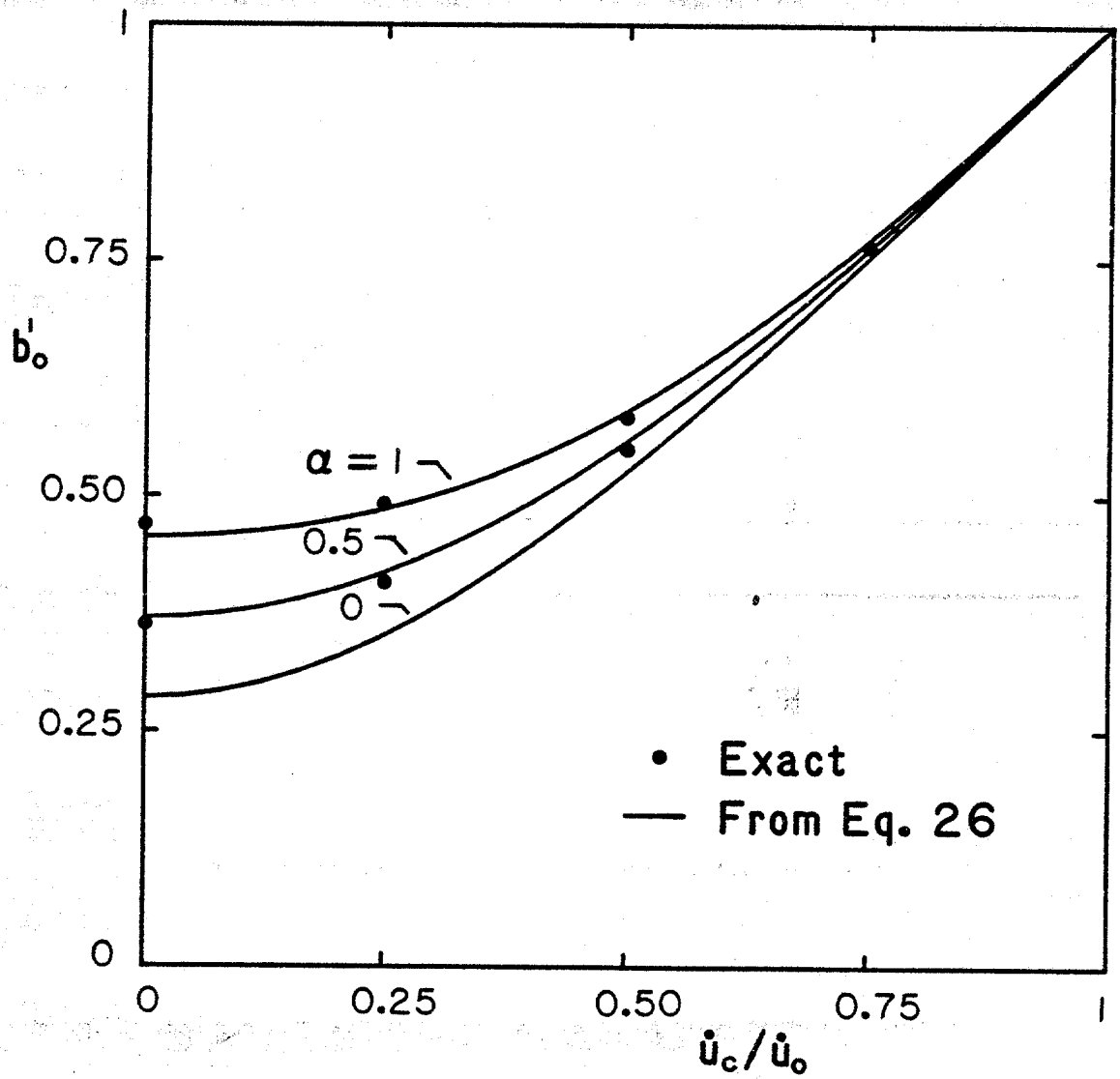


FIG. 11. Values of Proposed Damping Factor Coefficient,  $b'_0$

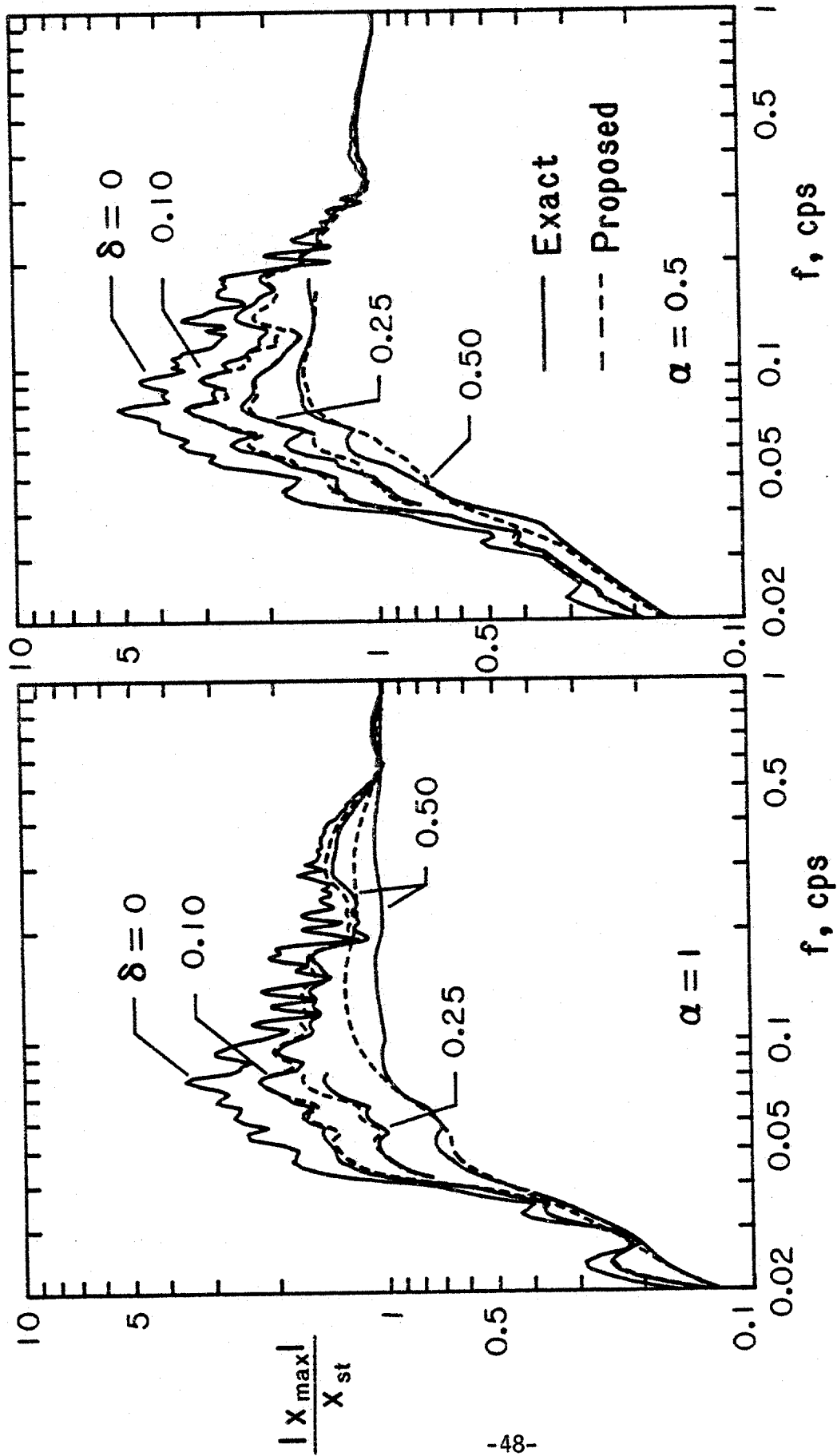


FIG. 12. Comparison of Response Spectra Computed by Exact Method and by Proposed Modification of Decoupling Technique; Interacting Systems with  $\zeta = 0.02$  Subjected to Wave Loading

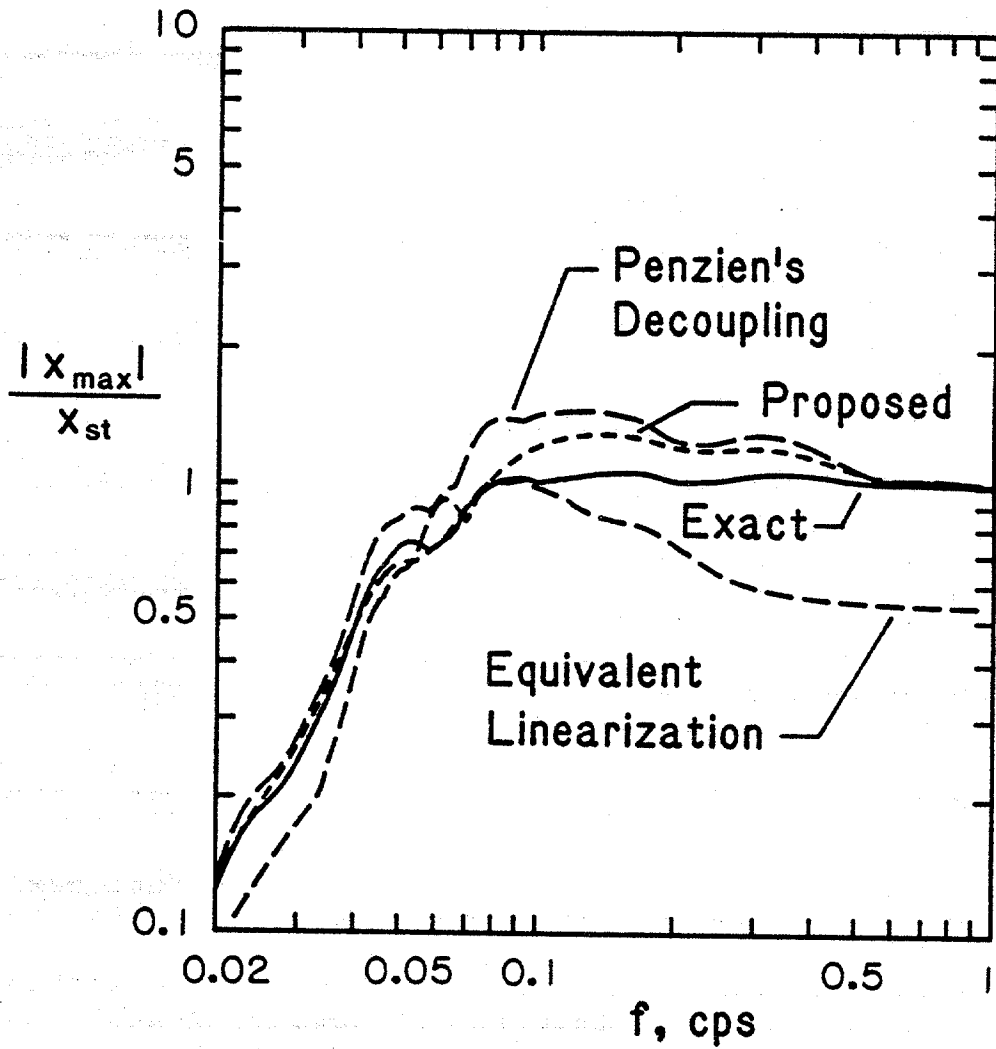


FIG. 13. An Extreme Comparison of Response Spectra Computed by Different Techniques; Systems with  $\delta = 0.50$ ,  $\zeta = 0.02$  and  $\alpha = 1$  Subjected to Wave Loading

U.S. DEPT. OF COMM. <b>BIBLIOGRAPHIC DATA SHEET</b> <i>(See instructions)</i>	<b>1. PUBLICATION OR REPORT NO.</b> NBS-GCR 86-519	<b>2. Performing Organ. Report No.</b>	<b>3. Publication Date</b> DECEMBER 1986
<b>4. TITLE AND SUBTITLE</b> <p style="text-align: center;">FLUID-STRUCTURE INTERACTION EFFECTS FOR OFFSHORE STRUCTURES</p>			
<b>5. AUTHOR(S)</b> <p style="text-align: center;">A. S. Veletsos, A. M. Prasad and G. Hahn</p>			
<b>6. PERFORMING ORGANIZATION</b> <i>(If joint or other than NBS, see instructions)</i> NATIONAL BUREAU OF STANDARDS DEPARTMENT OF COMMERCE WASHINGTON, D.C. 20234 A. S. Veletsos, Consultant 5211 Paisley Houston, TX 77096		<b>7. Contract/Grant No.</b> 41-USC-252-C3	<b>8. Type of Report &amp; Period Covered</b> FINAL REPORT
<b>9. SPONSORING ORGANIZATION NAME AND COMPLETE ADDRESS</b> <i>(Street, City, State, ZIP)</i> <p style="text-align: center;">Minerals Management Service          United States Department of the Interior          Reston, VA 22091</p>			
<b>10. SUPPLEMENTARY NOTES</b> <p><input type="checkbox"/> Document describes a computer program; SF-185, FIPS Software Summary, is attached.</p>			
<b>11. ABSTRACT</b> <i>(A 200-word or less factual summary of most significant information. If document includes a significant bibliography or literature survey, mention it here)</i> <p>Comprehensive analyses are made of the differences in the responses of simple models of offshore structures computed by the standard and extended versions of Morison's equation for the hydrodynamic forces, and of the effects and relative importance of the numerous parameters involved. The responses also are evaluated by the equivalent linearization technique and Penzien's decoupling technique, and the interrelationship and accuracy of these approaches are elucidated. The results are displayed graphically in the form of response spectra for absolute maximum displacement employing dimensionless parameters that are easy to interpret and use. In addition, the decoupling technique is generalized to include consideration of a current of constant velocity, and a simple modification is proposed which improves the accuracy of this approach. A particularly simple approximation is included for the hydrodynamic modal damping values of multi-degree-of-freedom, stick-like systems.</p>			
<b>12. KEY WORDS</b> <i>(Six to twelve entries; alphabetical order; capitalize only proper names; and separate key words by semicolons)</i> Hydrodynamics; loads; Morison's equation; offshore structures; structural engineering; waves			
<b>13. AVAILABILITY</b> <input checked="" type="checkbox"/> Unlimited <input type="checkbox"/> For Official Distribution. Do Not Release to NTIS <input type="checkbox"/> Order From Superintendent of Documents, U.S. Government Printing Office, Washington, D.C. 20402. <input checked="" type="checkbox"/> Order From National Technical Information Service (NTIS), Springfield, VA. 22161			<b>14. NO. OF PRINTED PAGES</b> 55 <b>15. Price</b> \$11.95